Human Immunology 80 (2019) 668–702

Contents lists available at ScienceDirect

Human Immunology

journal homepage: www.elsevier.com/locate/humimm

Mapping and definition of HLA class I and II serologic epitopes using an unbiased reverse engineering strategy

Fumiko Yamamoto[a,1], Lin Wang[a,1], Chia-Jung Chang[b], Dolly B. Tyan[a,c,*]

[a] Histocompatibility, Immunogenetics & Disease Profiling Laboratory, Stanford Blood Center, 3373 Hillview Avenue, Palo Alto, CA 94304, USA
[b] Stanford Genome Technology Center, 3165 Porter Drive, Palo Alto, CA 94304, USA
[c] Department of Pathology, Stanford University School of Medicine, 3373 Hillview Avenue, Palo Alto, CA 94304, USA

ARTICLE INFO

Keywords:
Epitope
HLA antibody
NGS
Algorithm
Transplantation

ABSTRACT

Current models describing HLA epitopes are both theoretical and empirical. Each has limitations yielding discordant results and increasingly complex modeling. The models make *a priori* assumptions that epitopes must be present only on the mature protein, solvent accessible, on the 'top' (peptide binding surface) of the molecule, restricted to the same class as the antibody, and in the same position on the target allele if reactive to more than one locus. Results obtained counter to these assumptions are routinely discounted. For the 17th International Histocompatibility and Immunogenetics Workshop, we developed a reverse engineering algorithm to define epitopes without these assumptions on a cohort of 332 primary transplant pairs. Complete NGS typing of the transcribed (including leader) genomic DNA for 11 HLA loci of donor and recipient and DSA assignment by single antigen beads was performed. Our results show that, when grouped by 16 class I and II allele specific DSA, uniform clusters and 172 specific amino acid target epitopes are recognized by recipients despite originating from disparate HLA pairs. Data also show that these targets can be in the leader, alpha 3, transmembrane and cytoplasmic domains, thus calling into question current assumptions regarding immunogenic epitopes. Comparisons of amino acid epitopes defined by the Terasaki and Duquesnoy groups (TerEp and EpRegistry) are given.

1. Introduction

Attempts to define epitopes leading to antibody production against HLA have spanned decades [1–11]; the models constrained by the tools and technology available at the time they were developed. These include cytotoxicity testing using polyclonal and multiparous sera, mouse and human monoclonals, serologically typed panels, a continuously evolving IMGT database, and more recently single antigen beads (SAB). Based on what could be tested, longstanding assumptions have been made influencing widely accepted models of today. These assumptions include that epitopes must be present only on the mature protein, solvent accessible, on the 'top' (peptide binding surface) of the molecule, restricted to the same class as the antibody (e.g., class I antibody can only have a class I epitope target, but not one in class II), and in the same position on the target allele if reactive to more than one locus [2,7,12,13]. As described more fully in the companion article by Chang in this issue, we developed an unbiased, reverse engineering software strategy to identify potential epitopes. Instead of looking (forward) at IMGT sequences for regions of polymorphism for putative epitopes, many of which have not been tested or proven by absorption/elution studies, we elected to have the computer inform us of potential epitopes using grouped DSA sets from primary transplant pairs with full length genomic NGS sequencing of donor and recipient, the latter tested by SAB for DSA. We made one assumption: a recipient would not make antibody to self, and one hypothesis: collecting multiple HLA disparate transplant pairs making the same DSA would lead to identifying essential epitope(s) shared among them. We did not restrict the algorithm in any way, except to scan triplets as the unit of choice, creating an overlapping triplet library by stepping through the entire full length protein one amino acid (AA) at a time starting with the first AA of the signal peptide (Met) for all 11 NGS typed loci. The results obtained are highly informative and call into question some assumptions and conclusions of current models.

* Corresponding author at: Histocompatibility, Immunogenetics & Disease Profiling Laboratory, Stanford University, 3373 Hillview Avenue, Palo Alto, CA 94304, USA.
E-mail address: dtyan@stanford.edu (D.B. Tyan).
[1] Shared first authors: Fumiko Yamamoto and Lin Wang contributed equally to this work.

https://doi.org/10.1016/j.humimm.2019.04.004
Received 8 January 2019; Received in revised form 19 March 2019; Accepted 7 April 2019
Available online 20 May 2019

2. Materials and methods

2.1. Transplant pairs

The IHIWS Epitope Component included samples from 332 primary transplant pairs (199 renal, 133 cardiac). Recipients of multi-organ transplants or with a history of pregnancy were excluded. Transfusion history was not assessed due to unreliability. Inclusion of pairs into this component of the workshop required complete data that comprised NGS typing (full length genomic for all exons) for 11 loci (A,B,C,DRB1,DRB3,DRB4,DRB5,DQA1,DQB1,DPA1,DPB1) for donor and recipient (alleles frozen at IMGT v3.25), and antibody/DSA assignment based on SAB results by IgG class I and II and Bio-C1q class I and II for each recipient.

2.2. Antibody testing

2.2.1. Pilot study and quality control

In preparation for the actual Epitope Component testing, a pilot study was performed by 13 volunteer labs including the Stanford core lab. A set of 5 PT samples and corresponding reagents and SOPs were sent to each laboratory including the sending laboratory and testing was performed using the same protocols and reagents as described below (except pilot used class II lot LS2A01 Lot 11). Data for the actual Epitope Component were included from every lab that passed the pilot project (80% consensus using defined cutoffs) without further QC testing, or from each laboratory not participating in the pilot study that had valid data on blinded controls sent to them and submitted with their antibody results as labeled unknowns. Pilot labs that did not meet the 80% cutoff could choose to submit data and include blind controls (that passed) or have the Stanford core lab perform testing to have their data included.

2.2.2. Workshop core data set

All sera were tested using the same lots of SAB for class I (LS1A04 Lot 7) and class II (LS2A01 Lot 12) from One Lambda, Inc.; Bio-C1q reagents were provided to all participants by Stanford. Results were analyzed in Fusion (Version 3.5). Standardized protocols, reagents and cutoffs were used and participants were expected to follow protocols precisely. Every serum was tested for IgG class I and II, and Bio-C1q class I and II. Stanford performed the C1q testing for labs that could not perform it but had all the other required NGS and IgG valid data and wanted their data included in the analysis. A total of 408 recipients were tested for antibody and 406 submitted to the workshop. Of these, 355 had valid NGS data for donor and recipient. Labs who did not submit successful blinded controls were then eliminated leaving a total number of 332 transplant pairs and 1328 tests having complete data. Sera included 82 pre- and 250 post-transplant samples where the patient was known to make DSA either pre- or post-transplant. The entire raw dataset we used for analysis can be found at http://dx.doi.org/10.17632/hwpts8srt9.1.

2.3. Cutoffs

For the pilot study, we used 1000 MFI as a cutoff for both IgG and C1q in order to assess concordance among the participating labs and determine a threshold of acceptability. Concordance scores over 80% were considered successful. For the analysis of the actual patient data submitted by all labs that passed QC, the IgG class I and II cutoffs were set to 1000 MFI for positive, and 500–999 for possible, whereas because each patient has a different background reactivity in the Bio-C1q assay, C1q cutoffs were set to 1000 MFI above the lower MFI value of the first breakpoint of ≥300 MFI for assignment of positive, and all values in between for possible.

2.4. DSA assignment

Some labs that successfully passed the pilot/QC did not follow the workshop scoring algorithm. Therefore, all results were reanalyzed by the Stanford Core Epitope group to assign the antibodies. Only DSA in the positive (not possible) range were analyzed for this study. The reactivity of each serum was then compared to the genotype list (GL) strings of the recipient and donor to assign the DSA by each method. Confirmation of the GL strings was also performed by Stanford in cases where the DSA did not match the donor allele.

2.5. Generation of triplet data

Data including transplant code, donor GL string, and recipient GL string were extracted as .csv files and converted to .txt files in groups by center. The software processed the .txt files for unbiased triplet scanning (see companion paper by Chang, this issue, for method) and the generated triplet data were imported into the IHIWS database. Unlike other epitope programs which only look at the mature protein, we scanned the entire transcribed protein and started triplet scanning beginning at the first AA of the first triplet (MET). Hence the positions of the AA in the triplets is offset by the length of the signal peptide and can have negative positions in the IMGT. The triplet start sites were at −24 (class I), −29 (DRB), −23 (DQA), and −32 (DQB). If GL strings were changed by the core (e.g., erroneous assignment by submitting lab), this process had to be repeated to create new triplet files. Once all data were reviewed and accurate, samples sharing the same DSA were grouped and searched for common triplets. Common triplets were extracted by transplant ID, triplet sequence, allele of origin, and position independently for both IgG and C1q DSA. We aligned the triplets in descending order by frequency and ascending order by position in the protein (e.g., Fig. S1). For the first pass, we looked at transplant pairs where the recipient made a single (preferably allele specific) DSA in a particular class, so that the grouping would not be influenced by other DSA or third party antibodies in the same class. To increase the numbers of pairs for any given DSA of interest, we then included pairs with reactivity to a whole antigen (e.g., DR4), and finally to those with multiple other DSA, each of which was analyzed separately.

2.6. Mapping

For class I, we mapped the single heavy chain and assigned it to the alpha chain. For class II DRB1 and DRB4, we mapped only to the beta chain, and for DQ we mapped to both the alpha and the beta chains. Using the common triplets found by the algorithm, we extended the triplets from the first AA of the first triplet to the last AA of the last triplet in a cluster so as not to bias how many of the AA in between form the epitope. We used the first AA of each triplet to map the triplets onto IMGT alignments to determine whether they coincided with polymorphic regions. For each DSA group, we aligned all recipient alleles from the same locus to the DSA target allele as the reference sequence to determine whether the triplets/clusters with less than 100% reactivity could be explained by shared sequence homology with the DSA target at a given position (i.e., self = nonreactive). We then narrowed down the actual target AA(s) being recognized within the clusters and compared these AA to epitopes listed as TerEP [12] and eplets in EpRegistry (EpR) (http://www.epregistry.com.br) [11,14,15]. Finally, we mapped distinct putative epitope clusters and target AA onto the closest existing HLA structures using iCn3D (https://www.ncbi.nlm.

Table 1
A*02:01.

Position from Start	IgG		C1q		AA Position	3D_Position	Group#	Epitope	Exon	3D_Color	TerEp	T-AAs
	N = 14	N = 5	N = 10	N = 4								
	Count_ALL	Count_ONLY	Count_ALL	Count_ONLY								
85	12	3	9	4	62	62–68	a1		exon2	Cyan	17	62G
87	12	4	9	3	64						201	62G + 66K
88	12	4	9	3	65						238	56G + 65R
89	**6**	**2**	**6**	**3**	66			**66K**				
97	13	**5**	**10**	**4**	74	74–76	a2	**74H**	exon2	White	201	62G + 76V
116	**14**	**5**	**10**	**4**	93	93–95	a3	**95V**	exon2	Green		
128	**14**	**5**	**10**	**4**	105	105–109	a4	**107W**	exon3	Green	2	W
129	**14**	**5**	**10**	**4**	106						2	W
130	**14**	**5**	**10**	**4**	107						2	W
135	**8**	**3**	**7**	**4**	112	112–116	a5	**114H,116Y**	exon3	Yellow		
136	**8**	**3**	5	3	113							
137	**8**	**3**	**7**	**4**	114							
148	**8**	**3**	**5**	**3**	125	125–129	a6	**127K**	exon3	White	19	K
149	**8**	**3**	**5**	**3**	126						19	K
150	**8**	**3**	**5**	**3**	127						19	K
164	**14**	**5**	**8**	**3**	141	141–147	a7	**142T,145H**	exon3	Cyan	18/412	142T + 149A
165	**14**	**5**	**8**	**3**	142						18/412	142T + 149A
166	**14**	**5**	**8**	**3**	143						18/412	142T + 149A
167	**14**	**5**	**8**	**3**	144						13	13K
168	**14**	**5**	**8**	**3**	145						145	145H
172	6	3	3	1	149	149–152	a8	***151H,152V***[a]	exon3	Gray	412/422	145H + 149A
173	**11**	**5**	**6**	**3**	150						412	145H + 149A

Reactivity

TX-Code	
IgG	**C1q**
N=14	**N=10**
	TX-Stan125
TX-Stan189	***TX-Stan189***
TX-Stan198	
TX-Stan203	**TX-Stan203**
TX-Stan209	**TX-Stan209**
TX-Stan221	
	TX-Stan237
TX-Stan274	
	Kid-poTX002
Kid-poTX010	**Kid-poTX010**
	WA6RD
WA9RD	
KT_22	
KT_35	
SA09	**SA09**
SA08	***SA08***
SA01	
13	

gray: A2 ONLY Class I DSA

Blank = unreactive

Bold: Uniformly positive when not to self.

[a] Required together.

nih.gov/Structure/icn3d/full.html) (*cf* Chang, this issue). We displayed these on the relevant chain and oriented them with respect to the peptide whenever possible for clarity. Clusters and AA that lie within the leader, transmembrane (TM) and cytoplasmic (Cyto) domains are not mapped because the 3D structures only account for the solvent accessible portions of the mature proteins.

3. Results

3.1. Pilot study and QC

Table S1 shows overall results from 13 labs in the pilot study for the five blinded sera. For IgG1 and IgG2, 13/13 labs performed (mostly) successfully on each of the sera with high concordance for every bead (Tables S2 and S3). However, only 5/13 labs performed successfully using C1q1 and C1q2 despite standard reagents, SOPs, and cutoffs (e.g., Tables S1, S4, S5). The reason for the lack of concordance for C1q testing is unknown but may have related to isolated international shipping events or labs not using the provided reagents and required SOP. Ultimately, nine labs with successful pilot or blind controls or data from the core lab, had data included in the Epitope Component.

3.2. Samples

Analysis of pairs submitted by each center with complete data and the samples with positive, possible, and DSA antibody by each test type, and using IgG *positive* antibodies as a baseline, we found 89% (192/216) of class I and 71% (158/222) of class II are C1q+. For DSA, 86% (77/90) of class I and 49% (93/188) of class II are C1q+, confirming that the class II antibodies/DSA appear less able to fix complement.

3.3. DSA grouping and mapping

Once DSA were identified, there were enough samples (≥5/group) to evaluate the potential epitopes for the following antigens/alleles: A*02:01, A68, B*08:01, C*07:02, DR4, DRB4*01:03, DQA1*01:01/:05, DQA1*01:02/:03, DQA1*03:01/:03, DQA1*05:01, DQA1*05:03/:05, DQB1*02:01, DQB1*05:01, DQB1*06:02/:03/:04/:09, DQB1*03:01/:04/:19, DQB1*03:02. IgG results allow comparison to previously published putative or known epitopes. Tables show the subjects, triplets, frequencies, AA positions, clusters, and target AA for each DSA group. Uniformly found clusters from the Epitope Component were color mapped onto the closest related 3D structure in iCn3D in both sphere and ribbon depictions. AA were mapped on the ribbon only and colored according to their cluster of origin. The three views altogether provide the clearest picture.

3.3.1. A2 (A*02:01)

Eighteen recipients had DSA to A*02:01 by IgG (n = 14), C1q (n = 10) or both (n = 2). (Tables 1, S6). Eight clusters were uniformly present. Target AA are 66K, 74H, 95V, 107W, 114H, 116Y, 127K, 142T, 145H, 151H, and 152V. Reaction patterns indicate 151H and 152V must act as a pair. Shared TerEP AA are 66K, 107W, 127K, 142T, 145H, and 151H. Other TerEp targeting 13K, 62G, 56G + 65R, and 149A were not supported by sequence alignments and some were not found at all. EpR identifies 66K, 95V, 107W, 114H, 116Y, 127K, 142T, 151H, 152V in common. Two EpR eplets contain 145H (144TKH, 145KHA) but these include other AA we did not find. 74H, uniformly present by reverse engineering, is described as a possible (cryptic) TerEP (5001) and not listed in EpR. Fig. 1 shows clusters 1–2 (66K, 74H), 7 (142T, 145H),

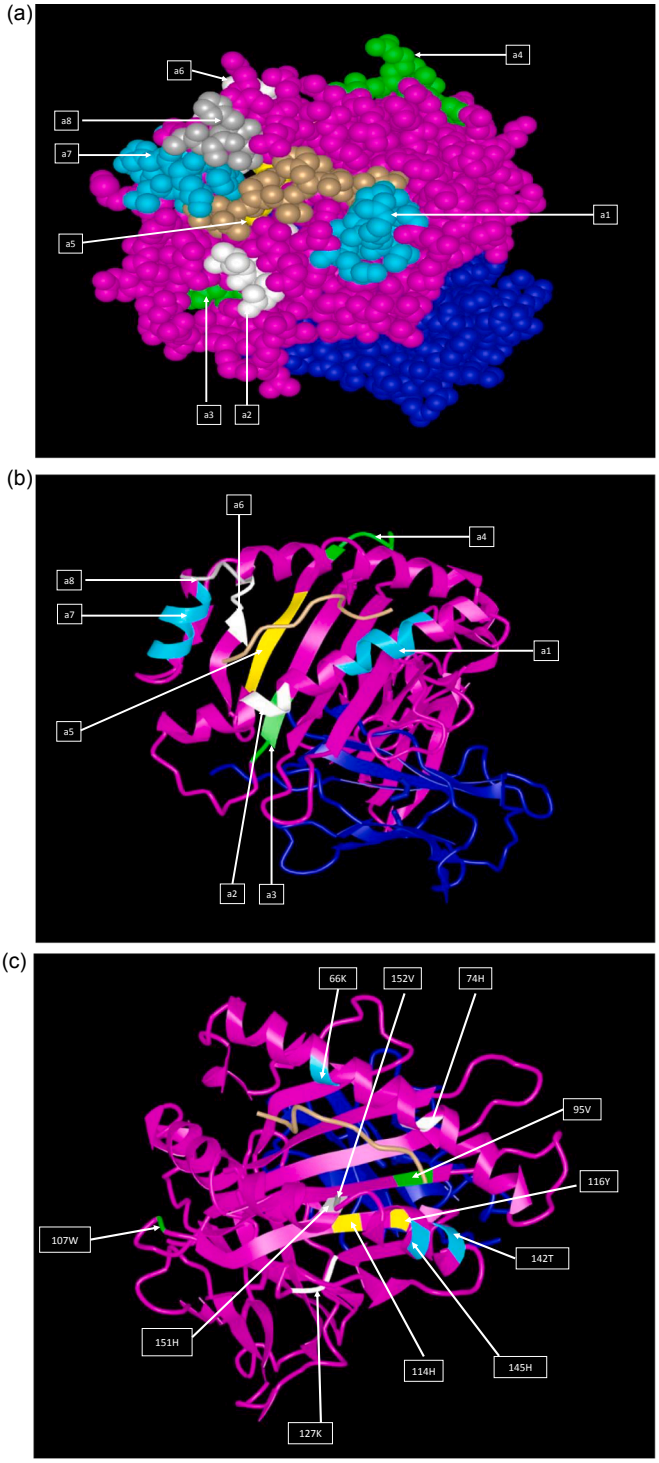

Fig. 1. Epitope mapping for A*02:01 showing (a) clusters mapped to alpha chain (pink), (b) clusters mapped to ribbon diagram, same orientation, and (c) individual AA targets mapped to ribbon diagram. Labels correspond to Table 1, and prefix letter in views (a) and (b) indicates chain.

and 8 (151H, 152V) are exposed on the alpha helices at each end of the groove, while clusters 3 (95V) and 5 (114H, 116Y) underlie the peptide on the beta pleated sheet, all potentially affecting peptide binding. Clusters 4 (107W) and 6 (127K) are on loops. Four of 11 target AA are histidine.

3.3.2. A68

Seven recipients had DSA to A68 (three A*68:01, two A*68:02, and two A*68:03) by IgG (Tables 2, S7). Five clusters were uniformly found. Target AA are 63N, 142T, 145H, 151H, 152V, 184A, and 245V. Again, 151H and 152V must act as a pair. Shared TerEp AA targets are 142T, 145H, and 151H, but 62R, 65R, 149A, and 150A are not found by our method. Our 184A and 245V have no TerEP equivalent, likely because these are encoded by exon 4. In EpR, complex eplets share 63N, 142T, and 145H, whereas 151H, 152V, 184A and 245V are described uniquely. Our data do not support the other AA targets in the complex eplets. Interestingly, A2 and A68 (same CREG group) share common epitopes of 142T, 145H, 151H, and 152V and Fig. 2 shows these,

Table 2
A*68.

Triplet	Position	IgG		AA Position	3D_Position	Group#	Epitope	Exon	3D_Color	TerEp	T-AAs
		N = 7 Count_ALL	N = 4 Count_ONLY								
NTR	86	**5**	**3**	63	63–65	a1	**63N**	exon2	Green	243	62R + 65R
QTT	164	**6**	**4**	141	141–147	a2	**142T,145H**	exon3	Cyan		
TTK	165	**6**	**4**	142						18	142T/145H
TKH	166	5	3	143							
KHK	167	**6**	**4**	144						13	144K
HKW	168	**6**	**4**	145						18	142T/145H
AHV	173	**5**	**3**	150	150–152	a3	***151H,152V***[a]	exon3	White	422	149A + 150A + 151H
TDA	205	**5**	**4**	182	182–186	a4	**184A**	exon4	Gray		
DAP	206	**5**	**4**	183							
APK	207	**5**	**4**	184							
KWV	**266**	**7**	**4**	243	243–246	a5	**245V**	exon4	Yellow		
WVA	**267**	**7**	**4**	244							

Reactivity

TX-Code
IgG
N=7
TX-Stan86
TX-Stan136
TX-Stan169
TX-Stan192
TX-Stan219
TX-Stan233
Kid-
poTX010

gray: A68 ONLY Class I DSA
Bold: Uniformly positive when not to self.
[a] Required together.

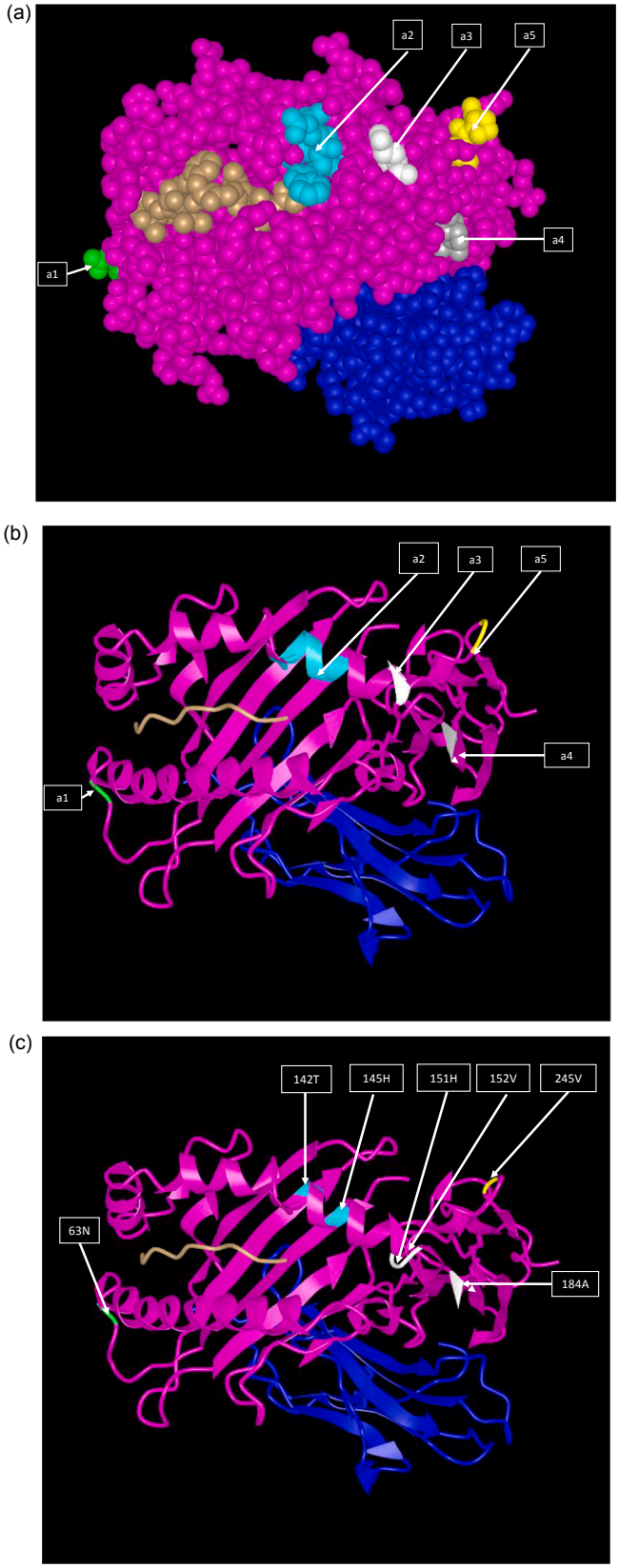

Fig. 2. Epitope mapping for A*68 showing (a) clusters mapped to alpha chain (pink), (b) clusters mapped to ribbon diagram, same orientation, and (c) individual AA targets mapped to ribbon diagram. Labels correspond to Table 2, and prefix letter in views (a) and (b) indicates chain.

together with 184A, reside in clusters 2–4 lying on one alpha helix, while clusters 1 (63N) and 5 (245V) are on remote and exposed loops at opposite ends of the groove.

3.3.3. B8 (B*08:01)

Seven recipients had DSA to B*08:01 by C1q (Tables 3, S8). Six clusters were uniformly found. Target AA are 67F, 97S, 116Y, 156D, 177D, 178T, 180E, and 325C. To explain the reactivity, 177D, 178T, 180E must be recognized together. TerEp share 177D and 180E in common. Multiple TerEp describe our cluster 1, but none identify 67F uniquely, which is noted as "not exposed at the surface of the HLA molecule" [12]. Other AA within these epitopes (65Q, 66I, 69T) cannot be explained by sequence. TerEP 420 (158A) is not found with our method since it looks like self in all but the two B38+ recipients. We did not find evidence for 109L + 131R (TerEP 205) defined by a mouse monoclonal. 97S, 116Y, 156D, 178T, and 325C have no TerEP equivalent and multiple other TerEp were not found. In EpR, unique and complex eplets include 67F, 97S, 116Y, 156D, 177D, 178T, 180E, but 325C is not listed. Our data do not support other AA listed in the complex eplets. Although we found 325C

Table 3
B*08:01.

Triplet	Position	C1q		AA Position	3D_Position	Group#	Epitope	Exon	3D_Color	TerEp	T-AAs
		N = 7 Count_ALL	N = 5 Count_ONLY								
QIF	88	**5**	**4**	65	65–69	a1	**67F**	exon2	Cyan	7, 225	65Q, 67F
IFK	89	**5**	**4**	66						225, 226	66I, 67F
FKT	90	**5**	**4**	67						11, 22, 225, 227, 420	67F, 69T
QSM	**119**	**6**	**5**	96	96–99	**a2**	**97S**	exon3	yellow		
SMY	**120**	**6**	**5**	97							
NQY	137	**5**	**4**	114	114–116	a3	**116Y**	exon3	White		
EQD	177	**6**	**4**	154	154–158	a4	**156D**	exon3	Green		
QDR	178	**6**	**4**	155							
DRA	179	**6**	**4**	156						420	158A
KDT	199	**6**	**4**	176	176–180	a5	***177D,178T,180E***[b]	exon3	Yellow		
DTL	200	**5**	3	177						11, 20	177D
TLE	201	**6**	**4**	178						11, 20	180E
CSD	348	**5**	**4**	325	325–327	a6	**325C**	exon7	N/A[a]		

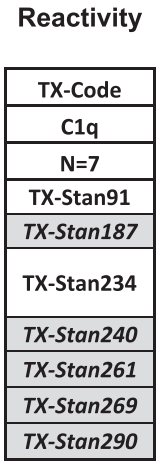

gray: B8 ONLY Class I DSA
Bold: Uniformly positive when not to self.
[a] N/A: Not apparent; cannot be displayed in 3D.
[b] Required together.

(encoded by exon 7) present in every pair with DSA to B8, it is missing from the other two systems based on their algorithms. Fig. 3 shows clusters 1 (67F) and 4 (156D) are centrally located on opposite alpha helices, straddling the peptide in the antigen binding groove, while clusters 2 (97S) and 3 (116Y) underlie the peptide in the beta sheet. Cluster 5 (177D, 178T, 180E) is remote and exposed. Cluster 6 (325C) cannot be mapped.

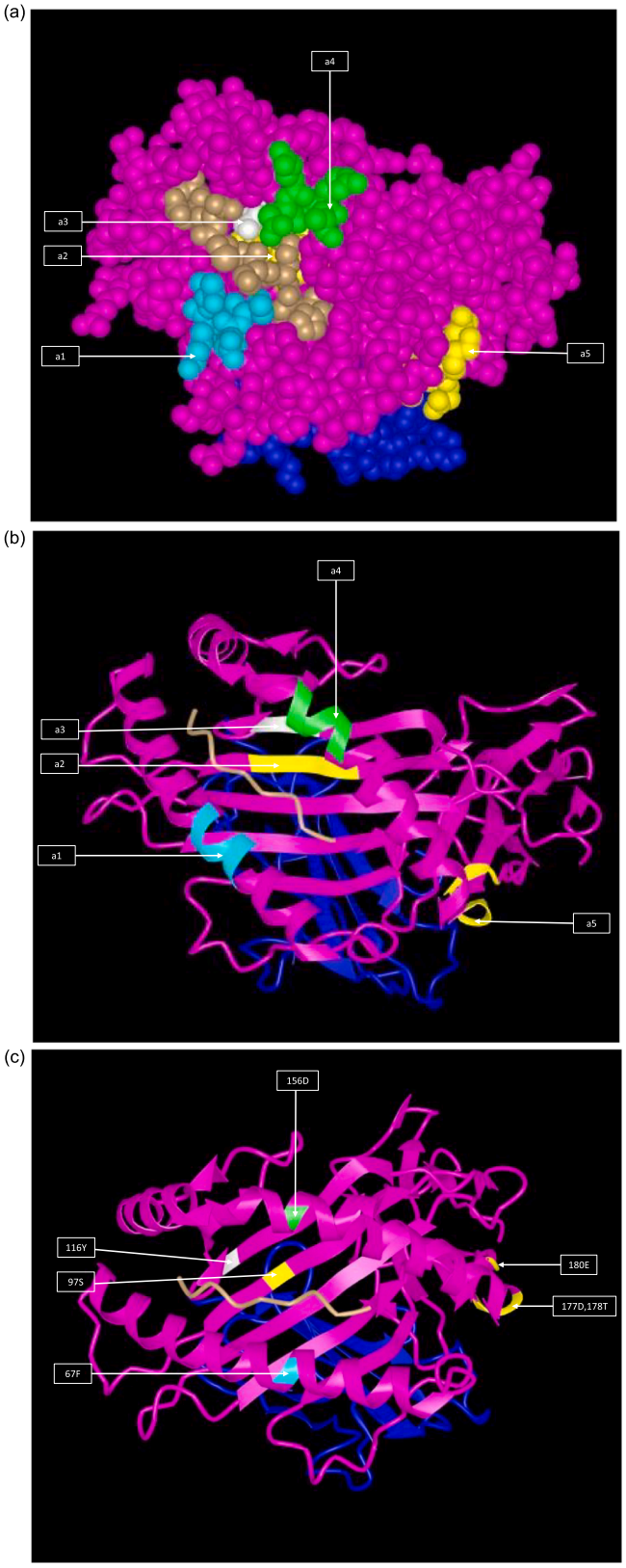

Fig. 3. Epitope mapping for B*08:01 showing (a) clusters mapped to alpha chain (pink), (b) clusters mapped to ribbon diagram, same orientation, and (c) individual AA targets mapped to ribbon diagram. Labels correspond to Table 3, and prefix letter in views (a) and (b) indicates chain.

3.3.4. Cw7 (C*07:02)

Eight recipients had DSA to C*07:02 by C1q (Tables 4, S9). Ten clusters were uniformly found. Target AA are 99S, 184P, 194L, 261M, 273S, 285M, 295V, 305T, 307M, 326C, 339T, and possibly 306A. With the exception of 194L (listed in TerEp) and 99S and 194L (listed in EpR), none of the others we found are listed in either system and our data support neither the additional AA in complex EpR eplets, nor other complex eplets. Notably, AA encoded by exons 3 and 4 provide only one target each, and the rest of the targets reside in locations encoded by exons 5–7. Despite being uniformly found, these targets, 285M, 295V, 305T, (306A?), 307M, 326C and 339T, would not be found in TerEp or EpR based on the assumptions of both models that only solvent exposed

Table 4
C*07:02.

Triplet		C1q		AA Position	3D_Position	Group#	Epitope	Exons	3D_Color	TerEp	T-AAs
	Position	N = 8 Count_ALL	N = 6 Count_ONLY								
RMS	120	**7**	**6**	97	97–101	a1	**99S**	exon3	Yellow		
MSG	121	**7**	**6**	98							
SGC	122	**7**	**6**	99							
AEP	205	**6**	**4**	182	182–185	a2	**184P**	exon4	Green		
EPP	206	**6**	**4**	183							
HPL	215	**6**	**4**	192	192–196	a3	**194L**	exon4	White	37	194L
PLS	216	**6**	**4**	193						37	194L
LSD	217	**6**	**4**	194						37	194L
CHM	282	**6**	**4**	259	259–263	a4	**261M**	exon4	Gray		
HMQ	283	**6**	**4**	260							
MQH	284	**6**	**4**	261							
TLS	294	**6**	**4**	271	271–275	a5	**273S**	exon4	Yellow		
LSW	295	**6**	**4**	272							
SWE	296	**6**	**4**	273							
PIM	306	**6**	**4**	283	283–286	a6	**285M**	exon5	N/A[a]		
IMG	307	**6**	**4**	284							
VLV	316	**6**	**4**	293	293–297	a7	**295V**	exon5	N/A[a]		
LVV	317	**6**	**4**	294							
VVL	318	**6**	**4**	295							
VVT	326	**6**	**4**	303	303–309	a8	**305T, 306A, 307M**	exon5	N/A[a]		
AMM	329	**6**	**4**	306							
MMC	330	**6**	**4**	307							
CSN	349	**6**	**4**	326	326–328	a9	**326C**	exon6	N/A[a]		
LIT	360	**6**	**4**	337	337–341	a10	**339T**	exon7	N/A[a]		
ITC	361	**6**	**4**	338							
TCK	362	**6**	**4**	339							

Reactivity

TX-Code
C1q
N=8
TX-Stan8
TX-Stan28
TX-Stan115
TX-Stan127
TX-Stan200
TX-Stan253
TX-Stan277
WA5RD

gray: Cw7 ONLY Class I DSA
Bold: Uniformly positive when not to self.
[a] N/A: Not apparent; cannot be displayed in 3D.

AA can be epitopes. Mapping the five external domain clusters uniformly present, (Fig. 4) shows only cluster 1 (99S) is proximal to the peptide, underlying it on the beta sheet. Clusters 2 (184P), 3 (194L), 4 (261M) and 5 (273S) are all remote from the peptide binding groove, exposed and, interestingly, found in the alpha 4 domain. Because only external domains are present in iCn3D, clusters 6–10 (285M to 339T) in the TM and Cyto domains cannot be mapped. Unlike the other class I DSA we evaluated, all of the target AA epitopes are displaced toward the C terminus of the molecule. No target is found in the alpha 1 or 2 domains.

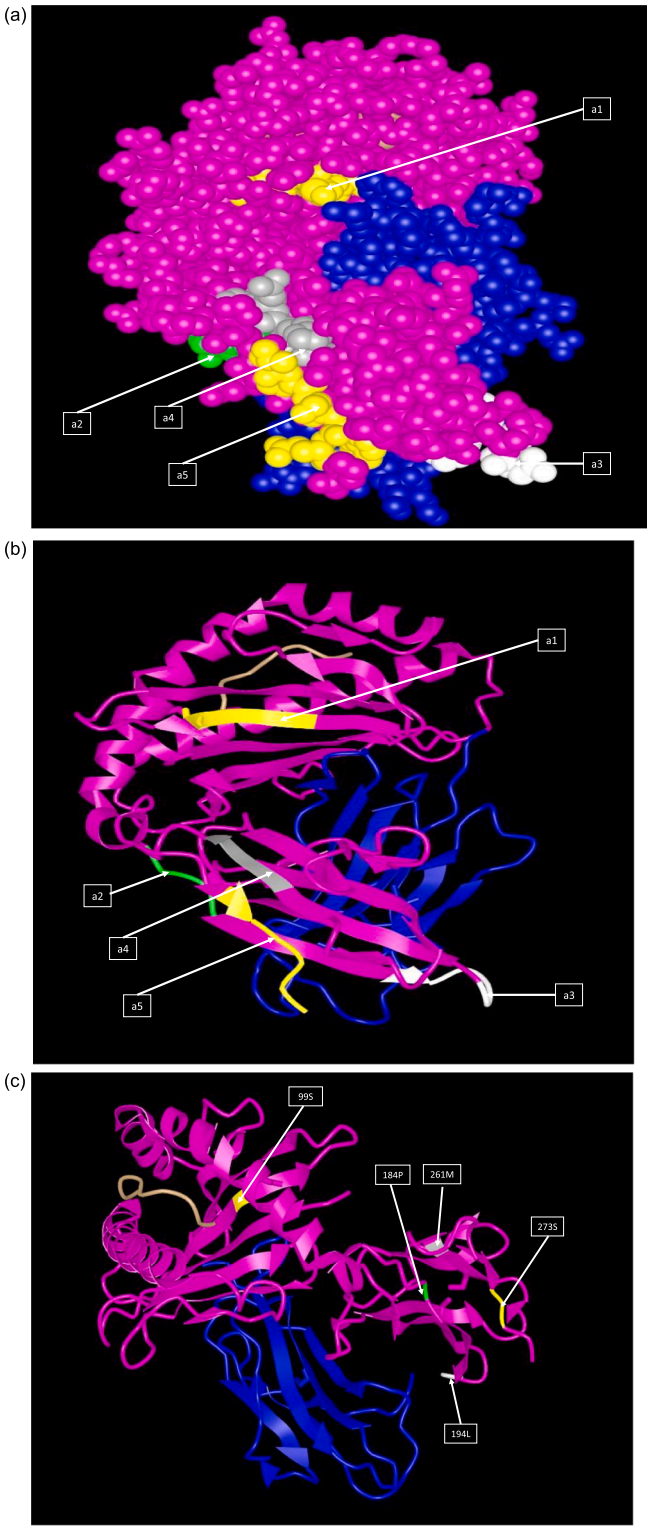

Fig. 4. Epitope mapping for C*07:02 showing (a) clusters mapped to alpha chain (pink), (b) clusters mapped to ribbon diagram, same orientation, and (c) individual AA targets mapped to ribbon diagram. Labels correspond to Table 4, and prefix letter in views (a) and (b) indicates chain.

3.3.5. DR4 (DRB1*04:01/:03/:04/:07)

Twenty-eight recipients had DSA to DR4 by IgG (Tables 5, S10). Six recipients were DR4+ making DSA to a mismatched DR4 allele. Recipients carrying a DR4 allele are eliminated from the total triplet counts (self) in our model when they share the same triplets. Four clusters were uniformly found in every DR4+ DSA. Target AA are −24F, 11V, 13H, 33H and 96Y. TerEp share 11V, 13H, 33H, and 96Y, but TerEP targets 10Q and 98E cannot be explained by reactivity. None of the epitopes, with the exception of 96Y (included in eplet $96Y_2$ with five other AA we did not find) is found in EpR. Two monoclonal antibodies (GS359-13F10 and NFLD.D1) are shown as confirming 96Y as an epitope. AA −24F is missing from both the TerEp and EpR systems

Table 5
DRB1*04:01/:03/:04/:07.

Triplet	Position	IgG		AA Position	3D_Position	Group#	Epitope	Exons	3D_Color	TerEP	T-AAs
		N = 28 Count ALL	N = 9 Count ONLY								
KFP	4	**22**	**8**	−25	−25 ~ −22	b1	**−24F**	exon1	N/A[a]		
FPG	5	**22**	**8**	−24							
EQV	37	**22**	**8**	9	9–15	b2	**11V, 13H**	exon2	Gray	1003	10Q
QVK	38	**22**	**8**	10						1003	10Q
VKH	39	**22**	**8**	11						1004	11V
KHE	40	**22**	**8**	12						1406	13H
HEC	41	**22**	**8**	13						1406	13H
FYH	59	**22**	**8**	31	31–35	b3	**33H**	exon2	Yellow	1605	33H
HQE	61	**22**	**8**	33						1605	33H
YPE	124	**22**	**8**	96	96–98	b4	**96Y**	exon3	Green	1034/1035	96Y/98E

Reactivity

TX-ID
N=28
TX-Stan14
TX-Stan29
TX-Stan42
TX-Stan43
TX-Stan45
TX-Stan55
TX-Stan80
TX-Stan132
TX-Stan138
TX-Stan139
TX-Stan166
TX-Stan168
TX-Stan169
TX-Stan189
TX-Stan207
TX-Stan212
TX-Stan225
TX-Stan227
TX-Stan228
TX-Stan233
TX-Stan251
TX-Stan252
TX-Stan257
TX-Stan267
TX-Stan284
SA13
2
17

gray: DR4 ONLY Class II DSA

Bold: Uniformly positive when not to self.

[a] N/A: Not apparent; cannot be displayed in 3D.

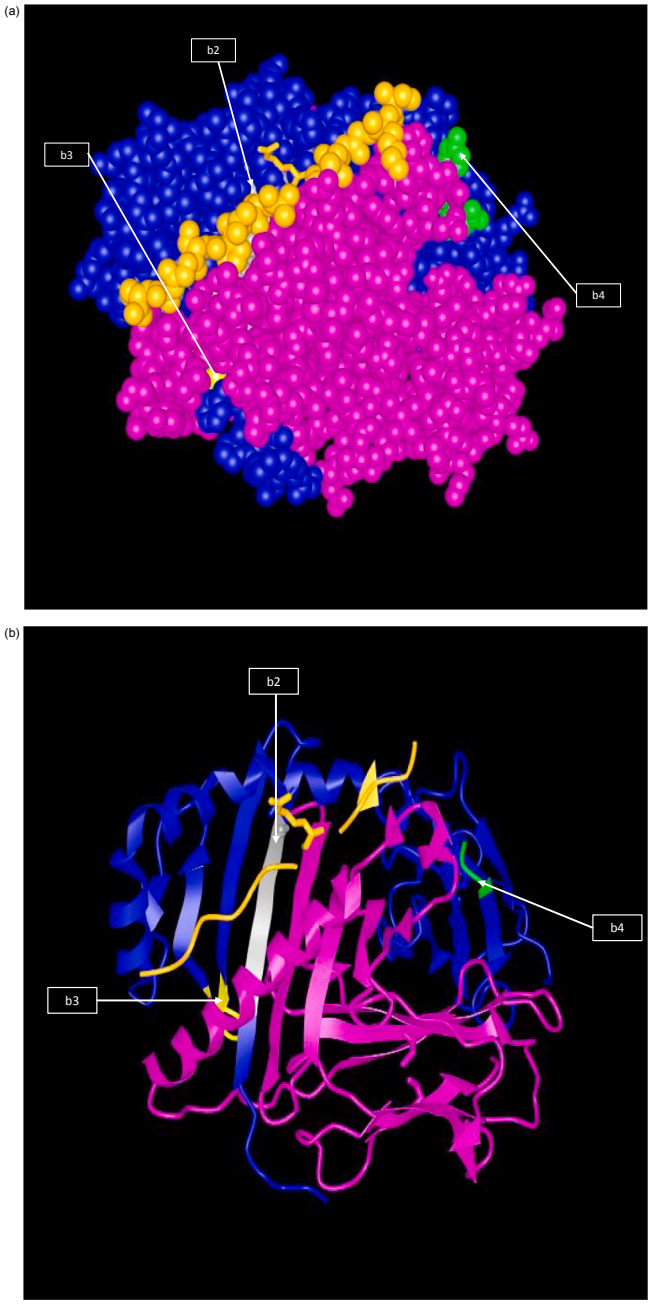

Fig. 5. Epitope mapping for DRB1*04 showing (a) clusters mapped to beta chain (blue), (b) clusters mapped to ribbon diagram, same orientation, and (c) individual AA targets mapped to ribbon diagram. Labels correspond to Table 5, and prefix letter in views (a) and (b) indicates chain.

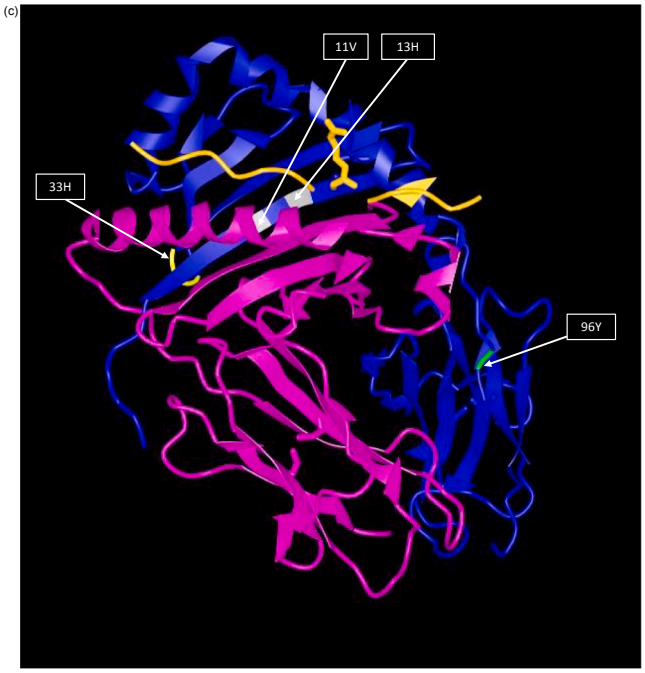

Fig. 5. (*continued*)

because leader encoded AA are not considered in these models. Fig. 5 shows that cluster 2 (11V, 13H) underlie the peptide on the beta sheet. Clusters 3 (33H) and 4 (96Y) are on loops at opposite ends of the groove. Cluster 3 may also partially underlie the peptide. Cluster 1 (-24F), in the leader, cannot be mapped because only mature proteins are present in iCn3D.

*3.3.6. DRB4*01:03*

Twenty-six recipients had DSA to DRB4*01:03 by IgG (Tables 6, S11). A single DRB4*01:03N recipient made DSA to the expressed DRB4*01:03 as expected. Seven clusters are uniformly observed. Target AA are 11A, 13C, 18L, 25W, 26N, 28I, 40Y, 41N, 44L, 48Q, 81Y, 180M, 181M, 187Q, 189S, 215T. TerEP shares only 40Y, but other TerEP targets, 10Q and 38A are not supported by our data. Eight reported TerEp associated with DR53 were not found in this DRB4*01:03 DSA set. In EpR, a single eplet ($48Q_6$) is comprised of 18L, 25W, 26N, 40Y, 41N, 44L, 48Q, 81Y and 180M. Even though we found 11A and 13C to be targets in all 26 DSAs to DRB4*01:03 from different transplant pairs, these are dismissed in EpR as being “in the peptide binding groove and unable to make direct contact with antibody.” EpR eplets 181M (confirmed) and 189S are both in common

Table 6
DRB4*01:03.

Triplet	Position	IgG		AA Position	3D_Position	Group#	Epitope	Exons	3D_Color	TerEp	T-AAs
		N = 26 Count ALL	N = 5 Count ONLY								
QAK	38	**26**	**5**	10	10–18	b1	**11A,13C,18L**	exon2	Yellow	1003	10Q
AKC	39	**26**	**5**	11							
KCE	40	**26**	**5**	12							
CEC	41	**26**	**5**	13							
HFL	44	**26**	**5**	16							
RVW	51	**26**	**5**	23	23–30	b2	**25W,26N,28I**	exon2	Red		
VWN	52	**26**	**5**	24							
WNL	53	**26**	**5**	25							
IRY	56	**26**	**5**	28							
ARY	66	**26**	**5**	38	38–50	b3	**40Y,41N,44L, 48Q**	exon2	Green	1014/1408	40Y/38A
NSD	69	**26**	**5**	41							
SDL	70	**26**	**5**	42							
LGE	72	**26**	**5**	44							
EYQ	74	**26**	**5**	46							
YQA	75	**26**	**5**	47							
QAV	76	**26**	**5**	48							
CRY	107	**26**	**5**	79	79–83	b4	**81Y**	exon2	Cyan		
YNY	109	**26**	**5**	81							
PSM	206	**26**	**5**	178	178–181	b5	**180M,181M**	exon3	White		
SMM	207	**26**	**5**	179							
VQW	214	25	**5**	186	186–189	b6	**187Q**	**exon3**	Gray		
QWS	215	**26**	**5**	187			**189S**	**exon4**			
GTG	242	**26**	**5**	214	214–216	b7	**215T**	exon4	N/A[a]		

Reactivity

TX-Code
IgG
N=26
TX-Stan21
TX-Stan103
TX-Stan123
TX-Stan138
TX-Stan148
TX-Stan169
TX-Stan172
TX-Stan189
TX-Stan197
TX-Stan198
TX-Stan212
TX-Stan213
TX-Stan222
TX-Stan271
TX-Stan274
TX-Stan290
Kid-poTX002
7298
WA11RD
KT_25
SA08
SA05
2
20
16
17

gray: DR53 ONLY Class II DSA
Bold: Uniformly positive when not to self.
[a] N/A: Not apparent; cannot be displayed in 3D.

with our data. Our epitopes 28I (encoded by exon 2), 187Q (exon 3), and 215T (exon 4) are not found in either of the other two systems. Fig. 6 shows clusters 1 (11A, 13C, 18L) and 2 (25W, 26N, 28I) underlie the peptide, while cluster 4 (81Y) is central on one alpha helix. These could influence what peptides are bound or their topography. Cluster 3 (40Y, 41N, 44L, 48Q) is at one end potentially influencing the n-terminal binding. Clusters 5 (180M, 181M) and 6 (187Q, 189S) are distant from the peptide but on exposed solvent accessible loops of the beta chain. Cluster 7 cannot be mapped.

*3.3.7. DQ2 (DQA1*05:01/DQB1*02:01)*

Twenty-two recipients had DSA to DQA1*05:01/DQB1*02:01 by

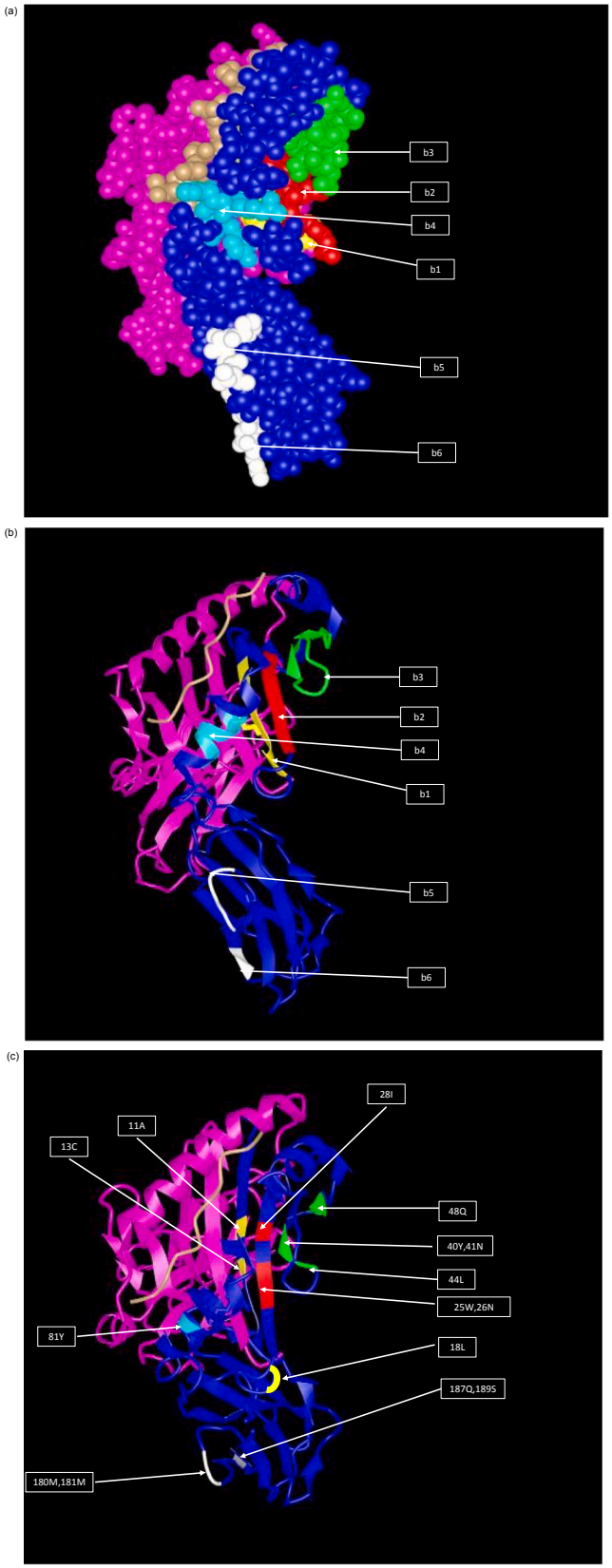

Fig. 6. Epitope mapping for DRB4*01:03 showing (a) clusters mapped to beta chain (blue), (b) clusters mapped to ribbon diagram, same orientation, and (c) individual AA targets mapped to ribbon diagram. Labels correspond to Table 6, and prefix letter in views (a) and (b) indicates chain.

IgG (n = 20), C1q (n = 12), or both (n = 7). Epitope clusters for DQA1*05:01 and DQB1*02:01 were analyzed separately and then merged for 3D representation.

*3.3.7.1. DQA1*05:01.* Six clusters were uniformly found (Tables 7, S12). Target AA are 40G, 47C, 50V, 51L, 53Q, 74S, 75L, 106I, 155L, 160E, 162S, and 174K. Notably, recognition of triplet 160E is only by

Table 7
DQA1*05:01.

Triplet	Position	IgG		C1q	AA Position	3D Positions	Group	Epitope	Exons	3D_color	TerEp	T-AAs
		N = 20 Counts ALL	N = 10 Counts ONLY	N = 12 Counts ALL/ONLY								
GRK	62	**16**	**6**	**9**	40	40–56	a1	**40G,47C,50V,51L,53Q**	exon2	Cyan	2018	40G
VWC	67	**16**	**6**	**9**	45						2018	47C
WCL	68	**16**	**6**	**9**	46						2018	47C
CLP	69	**16**	**6**	**9**	47						2018	47C
LPV	70	**16**	**6**	**9**	48							
VLR	72	**16**	**6**	**9**	50							
LRQ	73	**13**	**6**	7	51							
RQF	74	**16**	**6**	**9**	52							
QFR	75	**16**	**6**	**9**	53							
FRF	76	**16**	**6**	**9**	54							
LNS	94	**17**	**7**	**10**	72	72–75	a2	**74S,75L**	exon2	Gray		
NSL	95	**17**	**7**	**10**	73							
LIK	97	12	4	8	75							
KRS	99	8	4	7	77							
PNI	126	**17**	**7**	**10**	104	104–106	a3	**106I**	exon3	Yellow		
NIL	127	12	4	8	105							
ILI	128	12	4	8	106							
LLP	177	**17**	**7**	**10**	155	155–157	a4	**155L**	exon3	Green		
AEE	181	**17**	**7**	**10**	159	159–164	a5	**160E,162S**	exon3	White		
ESY	183	**17**	**7**	**10**	161							
SYD	184	**17**	**7**	**10**	162							
DKP	195	**17**	**7**	**10**	173	173–175	a6	**174K**	exon3	Yellow		

Reactivity

TX-Code	
IgG	C1q
N=20	N=12
TX-Stan1	*TX-Stan1*
TX-Stan3	
TX-Stan4	*TX-Stan4*
	TX-Stan9
TX-Stan79	
TX-Stan98	*TX-Stan98*
	TX-Stan141
TX-Stan170	
TX-Stan222	
TX-Stan240	*TX-Stan240*
TX-Stan247	
TX-Stan269	*TX-Stan269*
TX-Stan279	*TX-Stan279*
TX-Stan286	
10030	*10030*
6788	*6788*
P-10	
P-13	
WA2RD	*WA2RD*
C12345	
D12345	*D12345*
14	

gray: DQ2 ONLY Class II DSA

Blank = unreactive

Bold: Uniformly positive when not to self.

DQA1*05:01 DSA and not found in DSA to DQA1*05:03 or DQA1*05:05. However, DQA1*05:05+ recipients do not react with any of the listed targets (no DQA1*05:03+ recipients tested). A single TerEP (2018) is comprised of 40G and 47C in common, and no others are described. EpR lists $40GR_3$ comprising the group 40G, 47C, 50V, 51L, 53Q (our cluster 1), but lists six additional AA in this eplet that cannot account for the reactivity we observed. Only 40G is confirmed by absorption/elution studies. Four of the seven additional target AA we found, 74S, 75L, 160E, and 174K, are listed in EpR as 75S, 76L, 161E, and 175K, all offset by one AA residue. This is a consequence of an indel in DQA1*02, DQA1*04, and DQA1*05 immediately following AA 55 compared to DQA1*01 and DQA1*03, such that AA up to 55 are in the same position in both EpR and our data, but subsequently are displaced by one AA. The position after AA 55 depends on the reference sequence. We kept numbering of the residues consistent with the IMGT; in particular, since the numbering is the actual AA sequence of the DQA1*05 alleles. The three additional target AA we found (106I, 155L, 162S) are not present in the TerEP or EpR lists.

*3.3.7.2. DQB1*02:01:01.* Five clusters were uniformly found (Tables 8, S13). Target AA are −10S, 28S, 30S, 37I, 55L, 71K. Four DQB1*02:02+ recipients with DSA to DQB1*02:01 [by virtue of their

Table 8
DQB1*02:01.

Triplet	Position	IgG		C1q	AA Position	3D Positions	Group	3D_color	Epitope	Exons	TerEp	T-AAs
		N = 20 Counts_ALL	N = 10 Counts_ONLY	N = 12 Counts_ALL/ONLY								
LSM	21	**16**	**8**	**11**	−11	−11 ~ -8	b1	N/A[a]	**−10S**	**exon1**		
SML	22	**16**	**8**	**11**	−10							
LVS	57	11	5	7	26	26–32	b2	Yellow	**28S,30S**	**exon2**		
SRS	59	**16**	**8**	**11**	28						2001	28S/30S
RSI	60	**16**	**8**	**11**	29						2001	30S
SIY	61	**16**	**8**	**11**	30						2001	30S
EEI	66	**16**	**8**	**11**	35	35–39	b3	Green	**37I**	**exon2**	2001	37I
EIV	67	**16**	**8**	**11**	36						2001	37I
IVR	68	**16**	**8**	**11**	37						2001	37I
LPA	86	**16**	**8**	**11**	55	55–57	b4	Red	**55L**	**exon2**	2001	55L
RKR	101	**16**	**8**	**11**	70	70–72	b5	Gray	**71K**	**exon2**		

Reactivity

TX-Code	
IgG	C1q
N=20	N=12
TX-Stan1	*TX-Stan1*
TX-Stan3	
TX-Stan4	*TX-Stan4*
	TX-Stan9
TX-Stan79	
TX-Stan98	*TX-Stan98*
	TX-Stan141
TX-Stan170	
TX-Stan222	
TX-Stan240	*TX-Stan240*
TX-Stan247	
TX-Stan269	*TX-Stan269*
TX-Stan279	*TX-Stan279*
TX-Stan286	
10030	*10030*
6788	*6788*
P-10	
P-13	
WA2RD	*WA2RD*
C12345	
D12345	*D12345*
14	

gray: DQ2 ONLY Class II DSA

Blank = unreactive

Bold: Uniformly positive when not to self.

[a] N/A: Not apparent; cannot be displayed in 3D.

other mismatched allele(s)] share the corresponding triplets and were eliminated as self. One TerEP (2001) identifies 28S, 30S, 37I, 55L in common. EpR does not identify any AA we found, with the exception of 55L, included with 10 AA we did not find in eplet $45GE_3$. Other EpR DQB1*02:01 assigned eplets were not supported by our data. 71K is not listed by TerEP or EpR and neither model could have revealed −10S in the leader since the algorithms are restricted to the mature protein.

*3.3.7.3. DQA1*05:01/DQB1*02:01*. Combining the alpha and beta chain clusters, we observed prominent and likely interacting clusters at each end of the groove on the alpha helices. Fig. 7 shows clusters a1 (40G, 47C, 50V, 51L, 53Q), a2 (74S, 75L), b4 (55L), and b5 (71K)

Fig. 7. Epitope mapping for DQA1*05:01/DQB1*02:01 showing (a) clusters mapped to alpha (pink) and beta (blue) chains, (b) clusters mapped to ribbon diagram, same orientation, and (c) individual AA targets mapped to ribbon diagram. Labels correspond to Tables 7 and 8, and prefix letters in views (a) and (b) indicate chain.

exposed and tightly adjacent to the peptide whereas b2 (28S, 30S) and b3 (37I) underlie the peptide. Altogether, these would influence the peptides that could be bound. Clusters a3 (106I), a4 (155L), a5 (160E, 162S), and a6 (174K) are remote and exposed. Cluster b1 (leader) cannot be mapped. TerEp 2018 and 2001 support antibody recognition of AA in clusters a1, b2, b3 and b4.

3.3.8. DQ5 (DQA1*01:01/DQB1*05:01)

Nineteen recipients had DSA to DQA1*01:01/DQB1*05:01 (n = 18), DQA1*01:05/DQB1*05:01 (n = 1) by IgG (n = 14), C1q (n = 13), or both (n = 3). The alpha and beta chains were individually analyzed.

*3.3.8.1. DQA1*01:01/:05.* Seven clusters were uniformly found to DQA1*01:01/:05. (Tables 9, S14) Target AA are 11C, 18F, 45A, 47R, 48W, 50E, 52S, 53K, 55G, 61G, 66M, 69A, 76M, 80Y, 129Q, 218Q. No TerEp are described for DQA1*01. EpR has complex eplets ($41RA_2$, $52SK_5$) that include 18F, 45A, 52S, 53K, 55G, 66M, 69A, 80Y, and 129Q

Table 9
DQA1*01:01.

Triplet	Position	IgG		C1q		AA Position	3D Positions	Group	Epitope	Exons	3D color	TerEp	T-AAs
		N = 14 Counts ALL	N = 6 Counts ONLY	N = 13 Counts ALL	N = 11 Counts ONLY								
ASC	31	**10**	**5**	**10**	**10**	9	9–12	a1	**11C**	exon2	green		
SCG	32	**10**	**5**	**10**	**10**	10							
FYG	40	**10**	**5**	**10**	**10**	18	18–20	a2	**18F**	exon2	red		
TAW	66	**10**	**5**	**10**	**10**	44	44–62	a3	**45A,47R, 48W,50E, 52S,53K, 55G,61G**	exon2	white		
AWR	67	**10**	**5**	**10**	**10**	45							
WRW	68	**10**	**5**	**10**	**10**	46							
RWP	69	**10**	**5**	**10**	**10**	47							
WPE	70	**10**	**5**	**10**	**10**	48							
PEF	71	**10**	**5**	**10**	**10**	49							
EFS	72	**10**	**5**	**10**	**10**	50							
SKF	74	**10**	**5**	**10**	**10**	52							
KFG	75	**10**	**5**	**10**	**10**	53							
FGG	76	**10**	**5**	**10**	**10**	54							
GFD	78	**10**	**5**	**10**	**10**	56							
PQG	81	**10**	**5**	**10**	**10**	59							
QGA	82	**10**	**5**	**10**	**10**	60							
NMA	87	**10**	**5**	**10**	**10**	65	65–71	a4	**66M,69A**	exon2	cyan		
VAK	90	**10**	**5**	**10**	**10**	68							
AKH	91	**10**	**5**	**10**	**10**	69							
NIM	96	**10**	**5**	**10**	**10**	74	74–80	a5	**76M,80Y**	exon2	yellow		
IMI	97	**10**	**5**	**10**	**10**	75							
MIK	98	**10**	**5**	**10**	**10**	76							
KRY	100	**10**	**5**	**10**	**10**	78							
GQS	150	**12**	**6**	**12**	**11**	128	128–131	a6	**129Q**	exon3	green		
QSV	151	**12**	**6**	**12**	**11**	129							

(*continued on next page*)

Table 9 (*continued*)

Triplet	Position	IgG		C1q		AA Position	3D Positions	Group	Epitope	Exons	3D color	TerEp	T-AAs
		N = 14 Counts ALL	N = 6 Counts ONLY	N = 13 Counts ALL	N = 11 Counts ONLY								
IQG	239	**10**	**5**	**10**	**10**	217	217–218	a7	**218Q**	exon4	N/A[a]		
QGL	240	**10**	**5**	**10**	**10**	218							

Reactivity

TX-Code	
IgG	C1q
ALL: N=14	ALL: N=13
ONLY: N=6	ONLY: N=11
	TX-Stan40
	TX-Stan88
TX-Stan104	*TX-Stan104*
TX-Stan125	TX-Stan125
	TX-Stan134
TX-Stan157	
TX-Stan158	
TX-Stan190	
TX-Stan192	
TX-Stan213	
	TX-Stan253
TX-Stan261	*TX-Stan261*
	TX-Stan265
P-07	*P-07*
KT 92	
SA02	SA02
A12345	*A12345*
K12345	*K12345*
19	*19*

gray: DQ5 ONLY Class II DSA

Blank = unreactive

Bold: Uniformly positive when not to self.

[a] N/A: Not apparent; cannot be displayed in 3D.

in common. The seven additional AA we found are not listed and other EpR eplets assigned to DQA1*01:01 are not supported by our data. Of interest, 129Q is a target found only in DQA1*01:01 but not in DQA1*01:02 or DQA1*01:03 alleles.

*3.3.8.2. DQB1*05:01.* Twelve clusters were uniformly found for DQB1*05:01 (Tables 10, S15). Target AA are −27S, −21D, −9I, −5S, −4L, 14L, 26G, 30H, 53Q, 71A, 74S, 75V, 77R, 84E, 85V, 86A, 87Y, 89G, 90I, 116I, 125S, 182S, 220R, 221Q, 224R. Reaction patterns indicate 75V and 77R are recognized as a pair. Two complex TerEp

Table 10
DQB1*05:01.

Triplet	Position	IgG		C1q		AA Position	3D Positions	Group	Epitope	Exons	3D color	TerEp	T-AAs
		N = 14 Counts ALL	N = 6 Counts ONLY	N = 13 Counts ALL	N = 11 Counts ONLY								
KKS	3	**14**	**6**	**13**	**11**	−29	−29 ~ −27	b1	**−27S**	exon1	N/A[a]		
PGD	9	**12**	**5**	**12**	**10**	–23	–23 ~ −20	b2	**−21D**	exon1	N/A[a]		
GDL	10	**12**	**5**	**12**	**10**	–22							
LAI	21	**14**	**6**	**13**	**11**	−11	−11 ~ −2	b3	**−9I,-5S,-4L**	exon1	N/A[a]		
ILS	23	**14**	**6**	**13**	**11**	−9							
SSS	25	**14**	**6**	**13**	**11**	−7							
LAE	28	**12**	**5**	**12**	**10**	−4							
LCY	45	**14**	**6**	**13**	**11**	14	14–16	b4	**14L**	exon2	Green		

(*continued on next page*)

Table 10 (*continued*)

Triplet	Position	IgG		C1q		AA Position	3D Positions	Group	Epitope	Exons	3D color	TerEp	T-AAs
		N = 14 Counts ALL	N = 6 Counts ONLY	N = 13 Counts ALL	N = 11 Counts ONLY								
VRG	55	**11**	**6**	**8**	**6**	24	24–32	b5	**26G,30H**	exon2	Red		
RGV	56	**11**	**6**	**8**	**6**	25							
GVT	57	**11**	**6**	**8**	**6**	26							
TRH	59	**13**	**5**	**12**	**10**	28						2003	28T
RHI	60	**13**	**5**	**12**	**10**	29							
HIY	61	**13**	**5**	**12**	**10**	30							
PQG	83	**10**	**5**	**10**	**10**	52	52–54	b6	**53Q**	exon2	White	2003	52P
EGA	100	**14**	**6**	**13**	**11**	69	69–79	b7	**71A,74S, *75V,77R*** [b]	exon2	Cyan	2015	70G + 71A
GAR	101	**14**	**6**	**13**	**11**	70						2015	70G + 71A
RAS	103	**11**	**6**	**8**	**6**	72							
SVD	105	**11**	**6**	**8**	**6**	74							
VDR	106	**11**	**4**	**11**	**9**	75							
RVC	108	**9**	**4**	**6**	**4**	77							
YEV	114	**11**	**5**	**11**	**10**	83	83–92	b8	**84E,85V, 86A,87Y, 89G,90I**	exon2	Green	2004	84E/85V
EVA	115	**11**	**5**	**11**	**10**	84						2004	84E/85V
VAY	116	**14**	**6**	**13**	**11**	85						2004	85V
AYR	117	**14**	**6**	**13**	**11**	86						2004	86A
YRG	118	**14**	**6**	**13**	**11**	87						2004	89G
RGI	119	**11**	**5**	10	9	88						2004	90I
GIL	120	**11**	**5**	10	9	89						2004	90I
ILQ	121	**11**	**5**	**11**	**10**	90						2004	90I
LLI	145	**14**	**6**	**13**	**11**	114	114–118	b9	**116I**	exon3	White	2015	70G + 116I
ICS	147	**14**	**6**	**13**	**11**	116						2015	70G + 116I
PSQ	155	**14**	**6**	**13**	**11**	124	124–127	b10	**125S**	exon3	Gray	2015	70G + 125S
QSP	212	**9**	**3**	**9**	**8**	181	181–184	b11	**182S**	exon3	Red		
SPI	213	**9**	**3**	**9**	**8**	182							
IRQ	250	**11**	**5**	**11**	**10**	219	219–225	b12	**220R,221Q 224R**	exon4	N/A [a]	2004	221Q
RQR	251	**11**	**5**	**11**	**10**	220						2004	221Q
RSR	253	**14**	**6**	**13**	**11**	222							
SRK	254	**14**	**6**	**13**	**11**	223							

Reactivity

TX-Code	
IgG	C1q
ALL: N=14	ALL: N=13
ONLY: N=6	ONLY: N=11
	TX-Stan40
	TX-Stan88
TX-Stan104	*TX-Stan104*
TX-Stan125	TX-Stan125
	TX-Stan134
TX-Stan157	
TX-Stan158	
TX-Stan190	
TX-Stan192	
TX-Stan213	
	TX-Stan253
TX-Stan261	*TX-Stan261*
	TX-Stan265
P-07	*P-07*
KT 92	
SA02	SA02
A12345	*A12345*
K12345	*K12345*
19	*19*

gray: DQ5 ONLY Class II DSA

Blank = unreactive

Bold: Uniformly positive when not to self.

[a] N/A: Not apparent; cannot be displayed in 3D.

[b] Required together.

(2004, 2015) include 71A, 84E, 85V, 86A, 89G, 90I, 116I, 125S, and 221Q in common. EpR has unique and complex eplets that include 26G, 30H, 53Q, 71A, 74S, 75V, 77R, 84E, 85V, 86A, 87Y, 89G, 90I, 116I, 125S, 182S. Our data do not support 70G, listed by TerEP and EpR, due to reaction patterns that can only be explained by 71A, nor do our data support other TerEP "DQB5" or EpR DQB1*05:01 epitopes/eplets. Eight AA we identified, 5/9 (encoded by exon 1), 1/9 (exon 2), and 2/9 (exon 4) are not present in either of the other systems.

*3.3.8.3. DQA1*01:01/DQB1*05:01.* Fig. 8 shows that clusters a3 (45A,

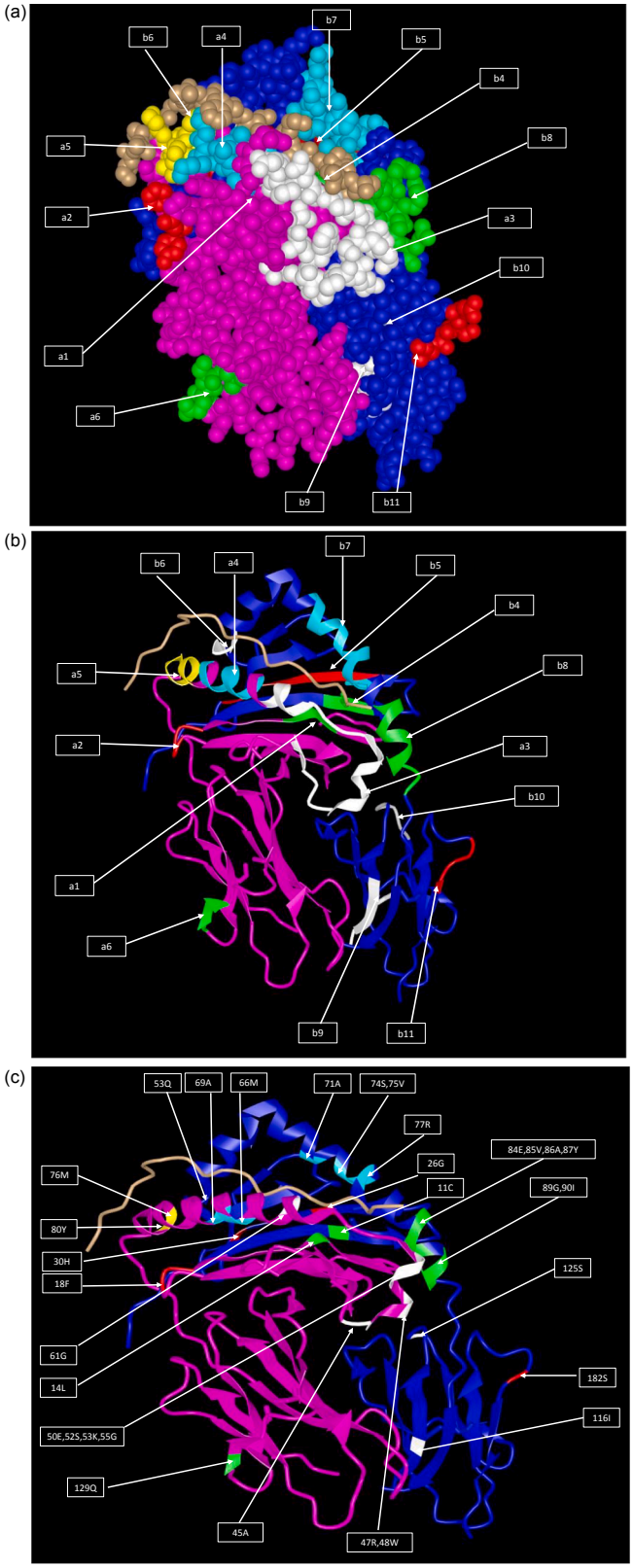

Fig. 8. Epitope mapping for DQA1*01/DQB1*05:01 showing (a) clusters mapped to alpha (pink) and beta (blue) chains, (b) clusters mapped to ribbon diagram, same orientation, and (c) individual AA targets mapped to ribbon diagram. Labels correspond to Tables 9 and 10, and prefix letters in views (a) and (b) indicate chain.

Table 10A
DQA1*01:02/:03.

Triplet	Position	IgG		C1q		AA Position	3D Position	Group	Epitope	Exons	3D-color
		N = 24 Counts ALL	N = 4 Counts ONLY	N = 10 Counts ALL	N = 7 Counts ONLY						
ASC	31	**16**	**3**	**8**	**6**	9	9–12	a1	**11C**	exon2	Green
SCG	32	**16**	**3**	**8**	**6**	10					
FYG	40	**16**	**3**	**8**	**6**	18	18–20	a2	**18F**	exon2	White
TAW	66	**16**	**3**	**8**	**6**	44	44–58	a3	**45A,47R, 48W,50E, 52S,53K, 55G**	exon2	Gray
AWR	67	**16**	**3**	**8**	**6**	45					
WRW	68	**16**	**3**	**8**	**6**	46					
RWP	69	**16**	**3**	**8**	**6**	47					
WPE	70	**16**	**3**	**8**	**6**	48					
PEF	71	**16**	**3**	**8**	**6**	49					
EFS	72	**16**	**3**	**8**	**6**	50					
SKF	74	**16**	**3**	**8**	**6**	52					
KFG	75	**16**	**3**	**8**	**6**	53					
FGG	76	**16**	**3**	**8**	**6**	54					
GFD	78	**16**	**3**	**8**	**6**	56					
PQG	81	**16**	**3**	**8**	**6**	59	59–62	a4	**61G**	exon2	Cyan
QGA	82	**16**	**3**	**8**	**6**	60					
NMA	87	**16**	**3**	**8**	**6**	65	65–71	a5	**66M,69A**	exon2	Yellow
VAK	90	**16**	**3**	**8**	**6**	68					
AKH	91	**16**	**3**	**8**	**6**	69					
NIM	96	**16**	**3**	**8**	**6**	74	74–80	a6	**76M,80Y**	exon2	Green
IMI	97	**16**	**3**	**8**	**6**	75					
MIK	98	**16**	**3**	**8**	**6**	76					
KRY	100	**16**	**3**	**8**	**6**	78					
IQG	239	**16**	**3**	**8**	**6**	217	217–220	a7	**218Q**	exon4	N/A[a]
QGL	240	**16**	**3**	**8**	**6**	218					

Reactivity

TX-Code	
IgG	C1q
N=24	N=10
TX-Stan60	
TX-Stan119	
TX-Stan144	
TX-Stan159	
	TX-Stan160
TX-Stan161	TX-Stan161
TX-Stan163	
TX-Stan205	
TX-Stan216	
TX-Stan218	*TX-Stan218*
TX-Stan221	
TX-Stan223	*TX-Stan223*
TX-Stan242	
	TX-Stan249
	TX-Stan281
P-01	
P-13	*P-13*
WA10RD	WA10RD
KT_1	
SA02	SA02
SA14	
11	
2	
3	
10	
15	*15*
18	

gray: DQ6 ONLY Class II DSA
Blank = unreactive

Bold: Uniformly positive when not to self.

[a] N/A: Not apparent; cannot be displayed in 3D.

Table 11
DQB1*06:02/:03/:04/:09.

Triplet	Position	IgG		C1q		AA Position	3D Position	Group	Epitope	Exons	3D-color	TerEp	T-AAs
		N = 24 Count_ALL	N = 4 Count_ONLY	N = 10 Count_ALL	N = 7 Count_ONLY								
PGD	9	**16**	**3**	**8**	**6**	–23	–23 ~ -20	b1	**−21D**	exon1	N/A[a]		
GDL	10	**16**	**3**	**8**	**6**	–22							
SLL	**26**	**18**	**3**	**8**	**6**	−6	−6 ~ -2	b2	***−6S,-5L,-4L***[b]	exon1	N/A[a]		
LLA	**27**	**18**	**3**	**8**	**6**	−5							
LAE	**28**	**18**	**3**	**8**	**6**	−4							
PQG	83	**16**	**3**	**8**	**6**	52	52–54	b3	**53Q**	exon2	Gray	2003	52P
YEV	114	**16**	**3**	**8**	**6**	83	83–92	b4	**84E,90I**	exon2	Cyan	2004	84E
EVA	115	14	2	6	5	84							
VAF	116	15	2	6	5	85						2004	85V
AFR	117	15	2	6	5	86						2004	86A
FRG	118	15	2	6	5	87							
RGI	119	**16**	**3**	**8**	**6**	88							
GIL	120	15	**3**	**8**	**6**	89						2004	89G
ILQ	121	**16**	**3**	**8**	**6**	90						2004	90I
PGQ	155	**20**	**3**	**8**	**6**	124	124–127	b5	**125G**	exon3	White		
GQI	156	**20**	**3**	**8**	**6**	125							
IRQ	250	**16**	**3**	**8**	**6**	219	219–222	b6	**220R, 221Q**	exon4	N/A[a]		
RQR	251	**16**	**3**	**8**	**6**	220						2004	221Q

Reactivity

TX-Code	
IgG	C1q
N=24	N=10
TX-Stan60	
TX-Stan119	
TX-Stan144	
TX-Stan159	
	TX-Stan160
TX-Stan161	TX-Stan161
TX-Stan163	
TX-Stan205	
TX-Stan216	
TX-Stan218	*TX-Stan218*
TX-Stan221	
TX-Stan223	*TX-Stan223*
TX-Stan242	
	TX-Stan249
	TX-Stan281
P-01	
P-13	*P-13*
WA10RD	WA10RD
KT_1	
SA02	SA02
SA14	
11	
2	
3	
10	
15	*15*
18	

gray: DQ6 ONLY Class II DSA
Blank = unreactive

Bold: Uniformly positive when not to self.
[a] N/A: Not apparent; cannot be displayed in 3D.
[b] Required together.

47R, 48W, 50E, 52S, 53K, 55G, 61G), a4 (66M, 69A), and a5 (76M, 80Y) are exposed on one alpha helix and juxtaposed to exposed clusters b7 (71A, 74S, 75V, 77R) and b8 (84E, 85V, 86A, 87Y, 89G, 90I) on the opposite helix, together essentially enclosing the peptide and would appear to be easily visible to antibody. Clusters a1 (11C), b4 (14L), and b5 (26G, 30H) underlie the peptide on the beta sheet and clusters a2 (18F) and b6 (53Q) lie on loops at one end of the groove, all potentially impacting the peptide. The remaining clusters a6 (129Q), b9 (116I), b10 (125S), b11 (182S) are remote on exposed loops. Clusters a7, b1-b3, and b12 cannot be mapped.

3.3.9. DQ6 (DQA1*01:02/:03 and DQB1*06:02/:03/:04/:09)

Twenty-seven recipients had DSA to DQB1*06:02, *06:03, *06:04, and/or *06:09 by IgG (24), C1q (10), or both (2). Another three had DSA to DQB1*06:01. Our algorithm clearly showed that common triplet identity could not be assigned when grouping the DQB1*06:01 DSA with the rest of the DQ6 DSA. Once the DQB1*06:01 DSA were removed from the group, target AA epitopes became clear and revealed that DQB1*06:01 is structurally dissimilar from the rest of the DQ6 proteins at 4/10 AA targets, all in the leader sequence, where it is identical to DQ2, DQ3, and DQ4. We, therefore, chose to analyze the triplets for all DQ6 DSA except DQB1*06:01 and the latter had too few representations (n = 3) to evaluate independently.

*3.3.9.1. DQA1*01:02/:03.* All clusters and target AA are identical to those found for DQA1*01:01, with the exception that 129Q is not a DQA1*01:02/:03 DSA target, as noted above (Tables 10A, S15A).

*3.3.9.2. DQB1*06:02/:03/:04/:09.* Six clusters were uniformly found for DQB1*06:02/:03/:04/:09 (Tables 11, S16). Target AA are −21D, −6S, −5L, −4L, 53Q, 84E, 90I, 125G, 220R, 221Q. It is clear from our data that AA −6S, −5L, and −4L are acting as a single target unit because −4L should not have reacted in DQB1*05+ recipients, but did so. TerEP 2004 shares 84E, 90I, and 221Q in common but our reactivity data do not support 85V, 86A, or 89G as targets, also included in 2004. Our remaining seven AA targets have no counterpart in the TerEP system. It seems likely that the TerEp are more specific to DQB1*06:01, which we did not analyze. EpR lists 53Q, 84E (confirmed), 90I and 125G in common, but the complex eplets include five other AA not supported by our data. Among these, EpR indicates that 52P/53Q and 84E/85V pair to create the epitope, but 52P and 85V are not supported by our data. Five of our AA epitopes (encoded by exons 1 and 4) are not found in TerEP or EpR listings.

*3.3.9.3. DQA1*01/DQB1*06:02.* Fig. 9 shows that clusters a3 (45A, 47R, 48W, 50E, 52S, 53K, 55G), a4 (61G), a5 (66M, 69A), and a6 (76M, 80Y) all reside on one alpha helix and clusters a3 and b4 (84E, 90I) are juxtaposed at one end of the groove on opposite sides. Cluster a1 (11C) underlies the peptide in the beta sheet. Clusters a2 (18F), b3 (53Q), and b5 (125G) are on exposed loops. Clusters a7, b1, b2, and b6 cannot be mapped.

3.3.10. DQ7 (DQA1*05:03/:05 and DQB1*03:01/:04/:19)

Thirty-eight recipients had DSA to DQ7 comprising various allele combinations of *DQA1*05:03/:05 and DQB1*03:01/:04/:19* by IgG (35), C1q (22), or both (17).

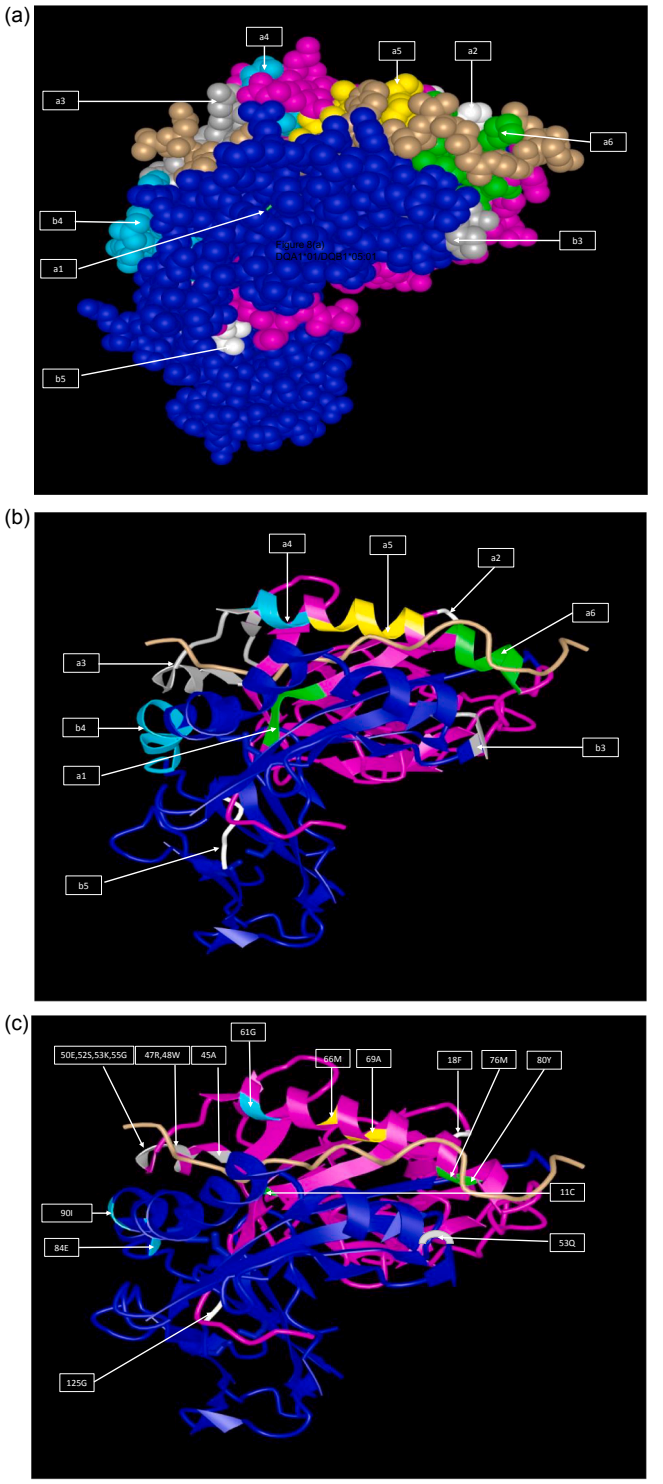

Fig. 9. Epitope mapping for DQA1*01/DQB1*06:02 showing (a) clusters mapped to alpha (pink) and beta (blue) chains, (b) clusters mapped to ribbon diagram, same orientation, and (c) individual AA targets mapped to ribbon diagram. Labels correspond to Tables 10A and 11, and prefix letters in views (a) and (b) indicate chain.

*3.3.10.1. DQA1*05:03/:05.* Six clusters were uniformly found (Tables 12, S17). Target AA are 40G, 47C, 50V, 51L, 53Q, 74S, 106I, 155L, 162S, 174K. Compared to DQA1*05:01, all target AA are the same except that 75L and 160E are not DSA targets for DQA1*05:03/:05 (*cf.* DQA1*05:01 description of TerEP and EpR targets).

Table 12
DQA1*05:03/:05.

Triplet	Position	IgG		C1q		AA Position	3D Position	Group	Epitope	Exons	3D-color	TerEp	T-AAs
		N = 35 Counts ALL	N = 11 Counts ONLY	N = 22 Counts ALL	N = 20 Counts ONLY								
GRK	62	**25**	**7**	**17**	**16**	40	40–56	a1	**40G,47C, 50V,51L, 53Q**	exon2	Gray	2018	40G
VWC	67	**25**	**7**	**17**	**16**	45						2018	47C
WCL	68	**25**	**7**	**17**	**16**	46						2018	47C
CLP	69	**25**	**7**	**17**	**16**	47						2018	47C
LPV	70	**25**	**7**	**17**	**16**	48							
VLR	72	**25**	**7**	**17**	**16**	50							
RQF	74	**25**	**7**	**17**	**16**	52							
QFR	75	**25**	**7**	**17**	**16**	53							
FRF	76	**25**	**7**	**17**	**16**	54							
LNS	**94**	**28**	**9**	**17**	**16**	72	72–75	a2	**74S**	exon2	White		
NSL	**95**	**28**	**9**	**17**	**16**	73							
PNI	**126**	**28**	**9**	**17**	**16**	104	104–106	a3	**106I**	exon3	Yellow		
LLP	**177**	**28**	**9**	**17**	**16**	155	155–157	a4	**155L**	exon3	Cyan		
ESY	**183**	**28**	**9**	**17**	**16**	161	161–164	a5	**162S**	exon3	Gray		
SYD	**184**	**28**	**9**	**17**	**16**	162							
DKP	**195**	**28**	**9**	**17**	**16**	173	173–175	a6	**174K**	exon3	Green		

Reactivity

TX-Code	
IgG	C1q
N=35	N=22
TX-Stan1	
TX-Stan2	*TX-Stan2*
TX-Stan10	*TX-Stan10*
TX-Stan11	*TX-Stan11*
	TX-Stan16
	TX-Stan21
TX-Stan24	*TX-Stan24*
TX-Stan25	*TX-Stan25*
TX-Stan27	
TX-Stan34	*TX-Stan34*
TX-Stan36	*TX-Stan36*
TX-Stan37	
TX-Stan38	
TX-Stan50	
TX-Stan52	
TX-Stan60	
TX-Stan79	*TX-Stan79*
TX-Stan147	*TX-Stan147*
TX-Stan171	
TX-Stan186	
TX-Stan205	
TX-Stan250	*TX-Stan250*
Kid-poTX002	Kid-poTX002
6482	*6482*
7050	*7050*
	7581
P-03	
P-16	
WA9RD	*WA9RD*
KT_34	*KT 34*
KT_32	*KT 32*
KT_19	*KT 19*
SA05	SA05
SA01	
SA03	*SA03*
I12345	
J12345	
14	

gray: DQ7 ONLY Class II DSA
Blank = unreactive
Bold: Uniformly positive when not to self.

*3.3.10.2. DQB1*03:01/:04/:19.* Seven clusters were uniformly present (Tables 13, S18). Target AA are 13A, 26Y, 45E, 52P, 57D, 140T, 167H, 182N. TerEp (2003, 2005, 2014) list 45E, 52P, and 182N in common. We did not find support for other AA targets in TerEp 2003, 2005, 2006, or 2008 because reactivity patterns cannot be explained by known sequences. Complex eplets in EpR list 26Y, 45E (confirmed), 52P, 57D,

Table 13
DQB1*03:01/:04/:19.

Triplet	Position	IgG		C1q		AA Position	3D Position	Group	Epitope	Exons	3D-color	TerEp	T-AAs
		N = 35 Count_ALL	N = 11 Count_ONLY	N = 22 Count_ALL	N = 20 Count_ONLY								
FKA	42	**28**	**10**	**17**	**16**	11	11–15	b1	**13A**	exon2	Yellow	2008	11F
KAM	43	**28**	**10**	**17**	**16**	12							
AMC	44	**28**	**10**	**17**	**16**	13							
RYV	56	**28**	**10**	**17**	**16**	25	25–28	b2	**26Y**	exon2	White		
YVT	57	**28**	**10**	**17**	**16**	26						2003	28T
DVE	74	**33**	**11**	**21**	**19**	43	43–46	b3	**45E**	exon2	Green	2005	45E
VEV	75	**33**	**11**	**21**	**19**	44						2003/2005	46V/45E
PLG	83	**21**	**8**	**17**	**15**	52	52–54	b4	**52P**	exon2	Yellow	2003	52P
PPD	86	**31**	**11**	**19**	**17**	55	55–57		**57D**			2006	55P
TTG	170	**21**	**8**	**17**	**15**	139	139–141	b5	**140T**	exon3	White		
PQH	196	**28**	**10**	**17**	**16**	165	165–169	b6	**167H**	exon3	Cyan		
QHG	197	**28**	**10**	**17**	**16**	166							
HGD	198	**28**	**10**	**17**	**16**	167							
LQN	211	**21**	**8**	**16**	**14**	180	180–184	b7		exon3	Green	2014	182N
QNP	212	**21**	**8**	**17**	**15**	181			**182N**				
NPI	213	**21**	**8**	**17**	**15**	182							

Reactivity

TX-Code	
IgG	C1q
N=35	N=22
TX-Stan1	
TX-Stan2	*TX-Stan2*
TX-Stan10	*TX-Stan10*
TX-Stan11	*TX-Stan11*
	TX-Stan16
	TX-Stan21
TX-Stan24	*TX-Stan24*
TX-Stan25	*TX-Stan25*
TX-Stan27	
TX-Stan34	*TX-Stan34*
TX-Stan36	*TX-Stan36*
TX-Stan37	
TX-Stan38	
TX-Stan50	
TX-Stan52	
TX-Stan60	
TX-Stan79	*TX-Stan79*
TX-Stan147	*TX-Stan147*
TX-Stan171	
TX-Stan186	
TX-Stan205	
TX-Stan250	*TX-Stan250*
Kid-poTX002	Kid-poTX002
6482	*6482*
7050	*7050*
	7581
P-03	
P-16	
WA9RD	*WA9RD*
KT_34	*KT 34*
KT_32	*KT 32*
KT_19	*KT 19*
SA05	SA05
SA01	
SA03	*SA03*
I12345	
J12345	
14	

gray: DQ7 ONLY Class II DSA
Blank = unreactive
Bold: Uniformly positive when not to self.

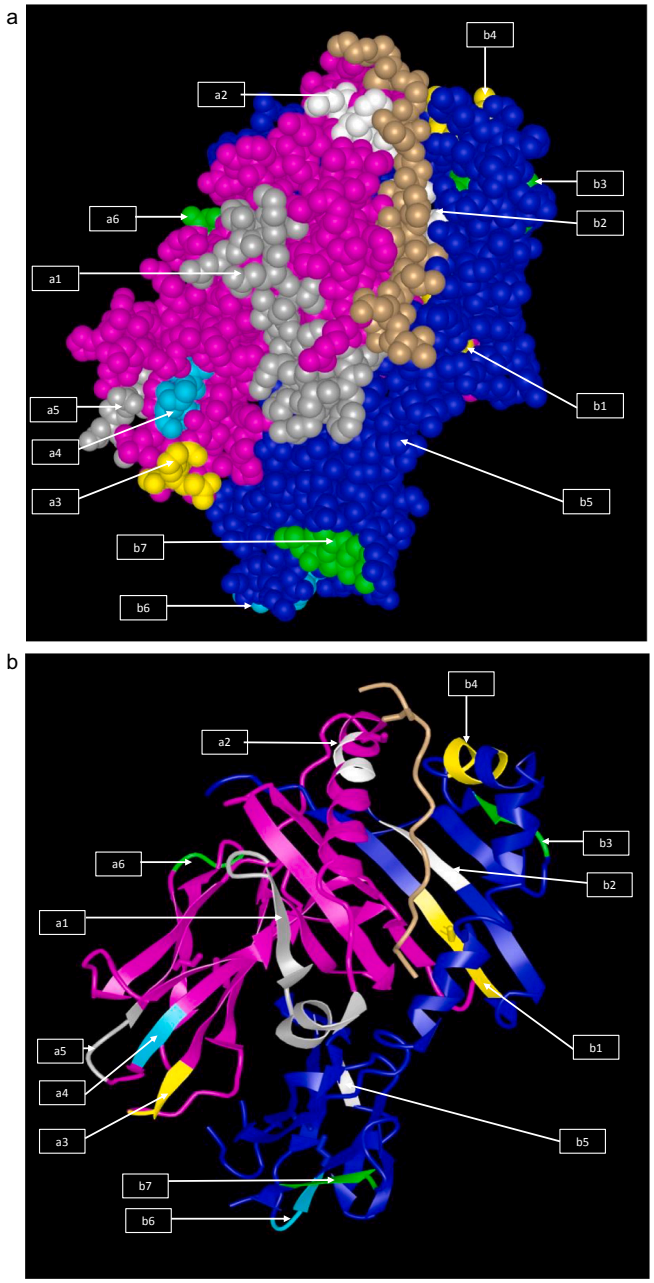

Fig. 10. Epitope mapping for DQA1*05/DQB1*03:01 showing (a) clusters mapped to alpha (pink) and beta (blue) chains, (b) clusters mapped to ribbon diagram, same orientation, and (c) individual AA targets mapped to ribbon diagram. Labels correspond to Tables 12 and 13, and prefix letters in views (a) and (b) indicate chain. In view (a) clusters hidden behind the molecule (e.g., b5) cannot be viewed in this orientation in the spherical representation but can be seen in view (b).

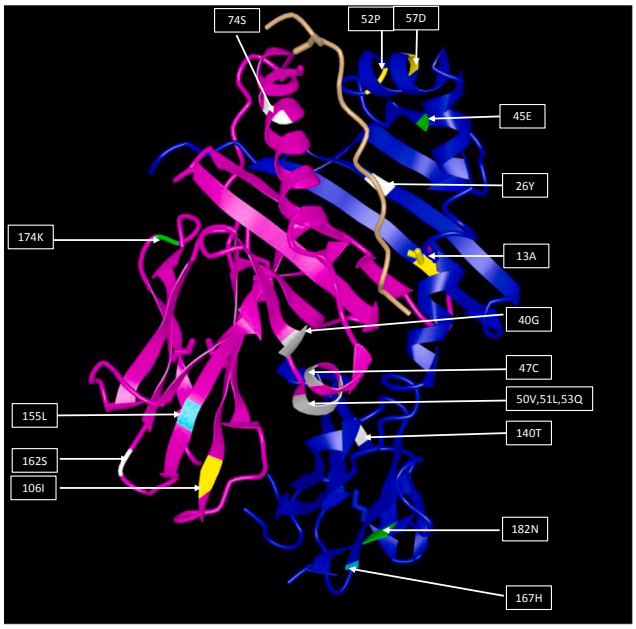

Fig. 10. (*continued*)

140T, 167H, 182N in common, plus a number of other AA we did not find. EpR also lists a number of other "confirmed" eplets ($46VY_3$, $52PL_3$, 55PP) corresponding to the TerEP AA we did not find, but no particular AA is confirmed. Neither of the other systems lists 13A (encoded by exon 2).

*3.3.10.3. DQA1*05/DQB1*03:01.* Fig. 10 shows that the epitope display of DQA1*05/DQB1*03:01 is similar to that for DQA1*05:01/DQB1*02:01. Cluster a1 (40G, 47C, 50V, 51L, 53Q) is a predominant epitope at one end of the groove while a2 (7S) and b4 (52P, 57D) lie on opposing alpha helices at the other end of the groove. Clusters b1 (13A) and b2 (26Y) underlie the peptide. Clusters a3-6 and b3, 5–7 are remote and exposed, with a3-a5 clustering together. Cluster b3 is away from the peptide on the back side of the beta chain. It is striking that so many target AA are remote from the peptide and clearly exposed. It is not clear if this contributed to the production of DQ7 DSA by so many recipients.

*3.3.11. DQ8 (DQA1*03:01/:03 and DQB1*03:02)*

Twelve recipients had DSA to DQB1*03:02 by IgG, 10 paired with DQA1*03:01 and two with DQA1*03:03.

*3.3.11.1. DQA1*03:01/:03.* Six clusters were uniformly found (Tables 14, S19). Target AA are 26S, 34E, 47Q, 50L, 53R, 56R, 76V, 175E, 187T. TerEP 2019 shares 26S, 47Q, 56R and 187T, but the five other AA epitopes we found are not described. EpR identifies 175E and a single unconfirmed eplet $47QL_5$ that includes 26S, 47Q, 50L, 53R, 56R, 76V, and 187T, in common with our findings. Seven other AA included in $47QL_5$ are not supported by our data. Neither TerEP nor EpR includes 34E (exon 2).

Table 14
DQA1*03:01/:03.

Triplet	Position	IgG Count_ALL (N = 12)	AA Position	3D_Position	Group	Epitope	Exons	3D-color	TerEp	T-AAs
QYS	46	**12**	24	24–28	a1	**26S**	exon2	Yellow		
YSH	47	**12**	25							
SHE	48	**12**	26						2019	26S
EFY	56	9	34	34–36	a2	**34E**	exon2	Cyan		
VWQ	67	**12**	45	45–57	a3	**47Q,50L, 53R,56R**	exon2	White	2019	47Q
WQL	68	11	46						2019	47Q
QLP	69	**12**	47						2019	47Q
LPL	70	11	48							
PLF	71	11	49							
LFR	72	**12**	50							
FRR	73	**12**	51							
RRF	74	**12**	52							
RFR	75	**12**	53							
FRR	76	**12**	54						2019	56R
RRF	77	**12**	55						2019	56R
NIV	96	**12**	74	74–78	a4	**76V**	exon2	Gray		
IVI	97	**12**	75							
VIK	98	**12**	76							
DEP	196	**11**	174	174–176	a5	**175E**	exon3	Cyan		
IPT	207	**12**	185	185–189	a6	**187T**	exon4	N/A[a]	2019	187T
PTP	208	**12**	186						2019	187T
TPM	209	**12**	187						2019	187T

Reactivity

TX-Code
IgG
N=12
TX-Stan138
TX-Stan148
TX-Stan166
TX-Stan189
TX-Stan198
TX-Stan212
TX-Stan225
TX-Stan278
KT_25
SA08
SA05
H12345

gray: DQ8 ONLY Class II DSA
Bold: Uniformly positive when not to self.
[a] N/A: Not apparent; cannot be displayed in 3D.

*3.3.11.2. DQB1*03:02.* A single cluster was uniformly found (Tables 15, S20), targeting 182N and 185I (encoded by exon 3). 182N is part of a complex TerEp (2014) but 185I is not found, and our data do not support the additional AA in TerEp 2014. Unique and complex EpR eplets list 182N and 185I in common, but these include other AA we did not find. Multiple other TerEP and EpR eplets attributed to 'DQB8' or DQB1*03:02 are not supported by our data, including TerEP 2006 and EpR 55PP, 55PPA, 55PPD, all targeting 55P, that cannot be explained by the reactivity we observed. Interestingly, this beta chain presents fewer epitopes than are observed for all other beta chains we could evaluate and differs substantially from DQB1*03:01, sharing only the 182N target.

Table 15
DQB1*03:02.

Triplet	Position	Count_ALL (N = 12)	AA Position	3D_Position	Group	Epitope	Exons	3D-color	TerEp	T-AAs
NPI	213	**7**	182	182–187	b1	**182N,185I**	exon3	Green		
PII	214	**11**	183						2014	182N
IVE	216	**11**	185							

Reactivity

TX-Code
IgG
N=12
TX-Stan138
TX-Stan148
TX-Stan166
TX-Stan189
TX-Stan198
TX-Stan212
TX-Stan225
TX-Stan278
KT_25
SA08
SA05
H12345

gray: DQ8 ONLY Class II DSA
Bold: Uniformly positive when not to self.

*3.3.11.3. DQA1*03/DQB1*03:02.* Fig. 11 shows cluster a3 (47Q, 50L, 53R, 56R) is a large epitope at one end of the peptide binding groove while a4 (76V) resides on the alpha helix at the other end. Clusters a1 (26S) and a2 (34E) underlie the peptide. Clusters a5 (175E), and b1 (182N, 185I) are remote and exposed. Cluster a6 could not be mapped. Notably, DQ8 has many fewer epitopes compared to the other DQ molecules we evaluated.

Fig. 11. Epitope mapping for DQA1*03/DQB1*03:02 showing (a) clusters mapped to alpha (pink) and beta (blue) chains, (b) clusters mapped to ribbon diagram, same orientation, and (c) individual AA targets mapped to ribbon diagram. Labels correspond to Tables 14 and 15, and prefix letters in views (a) and (b) indicate chain.

3.4. Epitope comparison

Table 16 compares the AA epitopes we found with those described by the other models. We found putative AA epitopes shared by all three, two of three, or unique to one. Reverse engineering defined 172 target AA, of which 47 (27.3%) are listed in TerEps, 110 (64.0%) are listed in EpR, and 38 (22.1%) shared by all three systems. If the 23 uniformly reactive target AA we found, encoded by exons missing from both other systems, are not included in the comparison since they would not have been found, then concordance for the remaining target AA (n = 149) in TerEp, EpR, and all three is 31.5%, 73.8%, and 25.5%, respectively.

Table 16a
CLASS I COMPARISON of TerEps, EpRegistry, and 17th IHIWS AMINO ACID EPITOPES.

		IHIWS AA	TerEp AA	EpR AA	TerEp	TerEp AA Not Found	EpR Eplet	EpR AA Not Found	Unreactive Recipient Alleles/Shared AA
1	A2 (A*02:01)	66K	√	√	201	43Q,62G,76V,79G	62GK,65RK,66K,66KA,66KH	62G,69A,70H,77D	A*23, A*24, A*34:01
		74H		√			62GK	62G,77D	
		95V		√			95V		
		107W	√	√	2		107W		
		114H		√			114H		A*23, A*24
		116Y		√			116Y		A*23, A*24
		127K	√	√	19		127K		A*23, A*24
		142T	√	√	18,412	(9F),149A,	144TKH	144K	
		145H	√	√	18,412	(9F),149A,	144TKH,145KHA	144K,149A	
		151HJ	√	√	422	149A,150A	149AH,150AAH,150AH,151AHV, 151H	149A,150A	A*24, A*68
		152V		√			151AHV,152V	150A	A*24, A*68
2	A68	63N		√			62RN	62R	
		142T	√	√	18		144TKH	144K	A*02
		145H	√	√	18		144TKH,145KHA	144K,149A	A*02
		151H	√	√	422	149A,150A	149AH,150AAH,150AH,151AHV, 151H	149A,150A	A*02,A*24:11N
		152V		√			151AHV,152V	150A	A*02,A*24:11N
		184A		√			184A		A*02,A*34
		245V		√			245V		
3	B8 (B*08:01)	67F	√	√	11, 225, 5085	131R,163T	66IF	66I	B*35
		97S		√			97S		B*07
		116Y		√			116Y		B*07,B*40,B*41,B*52,
		156D		√			156DA	158A	B*41
		177D	√	√	11,20		177DT		B*41
		178T		√			177DT		B*41
		180E	√	√	11,20		180E		B*41
		325C[b]							B*07,B*40,B*41
4	Cw7 (C*07:02)	99S		√	5039	66K	99S		
		184P							C*07:01
		194L	√	√	37		193PL	193P	C*07:01
		261M							C*07:01
		273S	√	√	5078		193PL	193P	C*07:01
		285M							C*07:01
		295V							C*07:01
		305T							C*07:01
		306A							C*07:01
		307M							C*07:01
		326C							C*07:01
		339T							C*07:01

Light gray rows indicate AA in the leader, transmembrane or cytoplasmic regions, and occasionally exon 4 encoded.

Table 16b
CLASS II – DR COMPARISON of TerEps, EpRegistry, and 17th IHIWS AMINO ACID EPITOPES.

		IHIWS AA	TerEp AA	EpR AA	TerEp	TerEp AA Not Found	EpR Eplet	EpR AA Not Found	Unreactive Recipient Alleles/Shared AA
5	DR4	-24F							DRB1*04 (any alternate allele)
		11V	√		1004, 1406				DRB1*04 (any alternate allele)
		13H	√		1406, 1605	180L			DRB1*04 (any alternate allele)
		33H	√		1605	180L			DRB1*04 (any alternate allele)
		96Y	√	√	1034, 1605	180L	$96Y_2$	98E,120N,180L,181T,183P	DRB1*04 (any alternate allele)
6	DR53 (DRB4*01:03)	11A							
		13C							
		18L		√			$48Q_6$		
		25W		√			$48Q_6$		
		26N		√			$48Q_6$		
		28I							
		40Y	√	√	1014, 1408	38A	$48Q_6$ $96QK_2$	96Q,98K, 120N	
		41N		√			$48Q_6$		
		44L		√			$48Q_6$		
		48Q		√			$48Q_6$		
		81Y		√			$48Q_6$		
		180M		√			$48Q_6$		
		181M		√			181M		
		187Q							
		189S		√			189S		
		215T							

Light gray rows indicate AA in the leader, transmembrane or cytoplasmic regions, and occasionally exon 4 encoded.

Table 16c
CLASS II – DQA1 COMPARISON of TerEps, EpRegistry, and 17th IHIWS AMINO ACID EPITOPES.

		IHIWS AA	TerEp AA	EpR AA	TerEp	TerEp AA Not Found	EpR Eplet	EpR AA Not Found	Unreactive Recipient Alleles/Shared AA
7	DQA1*01:01/05	11C							DQA1*01
		18F		√			$52SK_5$	56G,64R	DQA1*01
		45A		√			$41RA_2$, $52SK_5$	40E, 41R, 56G, 64R, 130S	DQA1*01
		47R							DQA1*01
		48W							DQA1*01
		50E							DQA1*01
		52S		√			$52SK_5$	56G,64R	DQA1*01
		53K		√			$52SK_5$	56G,64R	DQA1*01
		55G		√			$52SK_5$	56G,64R	DQA1*01
		61G							DQA1*01
		66M		√			$52SK_5$	56G,64R	DQA1*01
		69A		√			$52SK_5$	56G,64R	DQA1*01
		76M							DQA1*01
		80Y		√			$52SK_5$	56G,64R	DQA1*01
		129Q		√			$41RA_2$	40E, 41R, 130S	DQA1*01:01,DQA1*01:02, DQA1*01:05
		218Q							DQA1*01
8	DQA1*01:02/03	11C							DQA1*01,DQA1*06:01
		18F		√			$52SK_5$	56G,64R	DQA1*01
		45A		√			$41RA_2$, $52SK_5$	40E, 41R, 56G, 64R, 129Q,130S	DQA1*01
		47R							DQA1*01
		48W							DQA1*01
		50E							DQA1*01
		52S		√			$52SK_5$	56G,64R	DQA1*01
		53K		√			$52SK_5$	56G,64R	DQA1*01
		55G		√			$52SK_6$	56G,64R	DQA1*01
		61G							DQA1*01
		66M		√			$52SK_5$	56G,64R	DQA1*01
		69A		√			$52SK_6$	56G,64R	DQA1*01
		76M							DQA1*01
		80Y		√			$52SK_5$	56G,64R	DQA1*01
		218Q							DQA1*01
9	DQA1*03:01/03	26S	√	√	2019		$47QL_5$	25Y,48L,51F,52R,54F,55R,75I	
		34E							
		47Q	√		2019		$47QL_5$		
		50L		√			$47QL_5$	25Y,48L,51F,52R,54F,55R,75I	
		53R		√			$47QL_5$	25Y,48L,51F,52R,54F,55R,75I	
		56R	√	√	2019		$47QL_5$	25Y,48L,51F,52R,54F,55R,75I	
		76V		√			$47QL_5$	25Y,48L,51F,52R,54F,55R,75I	
		175E		√			175E		DQA1*04:01
		187T	√	√	2019		$47QL_5$	25Y,48L,51F,52R,54F,55R,75I	
10	DQA1*05:01	40G	√	√	2018		$40GR_3$	41R,45V,48L,52R,54F,55R	DQA1*04:01,DQA1*05:05
		47C	√	√	2018		$40GR_3$	41R,45V,48L,52R,54F,55R	DQA1*04:01,DQA1*05:05
		50V		√			$40GR_3$	41R,45V,48L,52R,54F,55R	DQA1*04:01,DQA1*05:05
		51L		√			$40GR_3$	41R,45V,48L,52R,54F,55R	DQA1*04:01,DQA1*05:05
		53Q		√			$40GR_3$	41R,45V,48L,52R,54F,55R	DQA1*04:01,DQA1*05:05
		74S		75S			$75S_3$,	163E	DQA1*05:05
		75L		76L			$75S_3$,76L	163E	DQA*02:01,DQA1*04,DQA1*05
		106I							DQA1*05:05
		155L							DQA1*05:05
		160E		161E			160AE	160A	DQA1*05:05
		162S							DQA1*05:05
		174K		175K			75S3	163E	DQA1*05:05
11	DQA1*05:03/05	40G	√	√	2018		$40GR_3$	41R,45V,48L,52R,54F,55R	DQA1*04,DQA1*05
		47C	√	√	2018		$40GR_3$	41R,45V,48L,52R,54F,55R	DQA1*04,DQA1*05
		50V		√			$40GR_3$	41R,45V,48L,52R,54F,55R	DQA1*04,DQA1*05
		51L		√			$40GR_3$	41R,45V,48L,52R,54F,55R	DQA1*04,DQA1*05
		53Q		√			$40GR_3$	41R,45V,48L,52R,54F,55R	DQA1*04,DQA1*05
		74S		75S			$75S_3$	76L,163E	DQA1*05
		106I							DQA1*05
		155L							DQA1*05
		162S							DQA1*05
		174K		175K			$75S_3$	76L,163E	DQA1*05

Light gray rows indicate AA in the leader, transmembrane or cytoplasmic regions, and occasionally exon 4 encoded.

Table 16d
CLASS II – DQB1 COMPARISON of TerEps, EpRegistry, and 17th IHIWS AMINO ACID EPITOPES.

		IHIWS AA	TerEp AA	EpR AA	TerEp	TerEp AA Not Found	EpR Eplet	EpR AA Not Found	Unreactive Recipient Alleles/Shared AA
12	DQB1*02:01	-10S							DQB1*02:02
		28S	√		2001	52L			DQB1*02:02
		30S	√		2001	52L			DQB1*02:02
		37I	√		2001	52L			DQB1*02:02
		55L	√	√	2001	52L	$45GE_3$	45G,46E,47F,52L,53L,56P,57A,74A,75V, 77R	DQB1*02:02
		71K							DQB1*02:02
13	DQB1*03:01/04/19	13A							DQB1*03:01,DQB1*03:04,DQB1*06:01
		26Y		√			$167H_2$		DQB1*03:01,DQB1*03:04,DQB1*06:01
		45E	√	√	2005		45EV	46V,47Y	DQB1*03:01,DQB1*03:04
		52P	√	√	2003	28T,46V	$46VY_3$, $52PL_3$, 55PP	28T,46V,47Y,53L,55P,56P	DQB1*03,DQB1*04:02
		57D		√			55PPD,56PD	55P,56P	DQB1*03:01,DQB1*03:03
		140T		√			$52PL_3$	53L	DQB1*03,DQB1*04:02
		167H		√			$167H_2$		DQB1*03:01,DQB1*03:04,DQB1*06:01
		182N	√	√	2014	77T,84Q,85L,86E, 87L	$52PL_3$	53L	DQB1*03,DQB1*04:02
14	DQB1*03:02	182N	√	√	2014	77T,84Q,85L,86E, 87L	$52PL_3$	52P,53L,140T	DQB1*03:03,DQB1*04:02
		185I		√			185I		
15	DQB1*05:01	-27S							
		-21D							DQB1*06:02,DQB1*06:03
		-9I							
		-5S							
		-4L							DQB1*06:02,DQB1*06:03
		14L							
		26G		√			$74SV_2$		DQB1*04:02
		30H		√			30H		DQB1*06:03
		53Q		√			$52PQ_2$	52P,55R,56P, 86G	DQB1*06
		71A	√	√	2015		$74SR_3$		
		74S		√			$74SR_3$,$74SV_2$		DQB1*04:02
		75V		√			$74SV_2$75V,77R		DQB1*02,DQB1*04:02
		77R		√			$74SR_3$,77R		DQB1*02,DQB1*04:02
		84E	√	√	2004		$52PQ_2$85VA	52P,55R,56P, 86G	DQB1*06
		85V	√	√	2004		$52PQ_2$ 85VA,85VY	52P,55R,56P ,86G	DQB1*06
		86A	√	√	2004		85VA		DQB1*06
		87Y		√			85VY		
		89G	√	√	2004		85VA,85VY		DQB1*06
		90I	√	√	2004		$52PQ_2$	52P,55R,56P, 86G	DQB1*06
		116I	√	√	2015		$74SR_3$		
		125S	√	√	2015		$74SR_3$,125SQ	126Q	
		182S		√			$140A_2$	140A	DQB1*06
		220R							DQB1*06:01,DQB1*06:03
		221Q	√		2004				DQB1*06:01,DQB1*06:03
		224R							
16	DQB1*06:02/03/04/09	-21D							DQB1*05,DQB1*06 (except *06:01)
		69							DQB1*05,DQB1*06 (except *06:01)
		74L							DQB1*05,DQB1*06 (except *06:01)
		74L							DQB1*05,DQB1*06 (except *06:01)
		53Q		√			$52PQ_2$	52P,55R,56P, 85V,86G	DQB1*05,DQB1*06
		84E	√	√	2004	85V,86A,89G,	$52PQ_2$ 85VA ,87F	52P,55R,56P, 85V,86G,86A,87F,89G	DQB1*05,DQB1*06
		90I	√	√	2004	85V,86A,89G,	$52PQ_2$	52P,55R,56P, 85V,86G,	DQB1*05,DQB1*06
		125G		√			125G		DQB1*06
		220R							DQB1*05,DQB1*06
		221Q	√		2004	85V,86A,89G,			DQB1*05,DQB1*06

Italics and speckled background indicate AA being recognized together.
Light gray rows indicate AA in the leader, transmembrane or cytoplasmic regions, and occasionally exon 4 encoded.

4. Discussion

Multiple approaches have been taken to define HLA epitopes leading to antibody formation. More recently these include theoretical (Duquesnoy), empirical (Terasaki), or both (Kosmoliaptsis [16,17]) models. Increasingly complex models evolved as technology advanced and data inconsistent with the models were found. Initially, the HLA epitope concept seemed simple with Bw4/Bw6 being a prime example; essentially a serologic dimorphism predating molecular sequences, now evolved to electrostatic potentials [17]. The MatchMaker model, as a theoretical prototype, has evolved from triplets, to patches, to eplets, to 'nonself-self', to antigenicity vs immunogenicity concepts in an attempt to explain outlier reactivity seen by various techniques. Concepts such as 'functional' and 'structural' epitopes have been hypothesized to attempt to correlate antibody paratope characteristics with predefined hypothetical epitopes. None are able to fully explain the observed data. In contrast, epitopes mapped by the Terasaki group are a compilation of results from mouse monoclonals and polyclonal multiparous or transfused human sera, the latter absorbed and eluted on recombinant/transfected cell lines, all tested on SAB. Critical information on responder and/or immunizer allele types is frequently missing from both models making it difficult to determine specificity. Further, there is no agreed upon definition of what (or how large) an epitope is (e.g., an immunogenic "eplet" vs a structural epitope), described as ranging in size from 3 Å to 850 Å. For our study, 'epitope' refers to a commonly recognized target region of ≥1 AA recognized by recipients making DSA to the same antigen/allele.

The two most widely used models defining HLA antibody inducing epitopes are based primarily on the excellent work by the Terasaki and Duquesnoy groups. Similarities and substantial differences exist between the two in epitopes identified and both make *a priori* assumptions based on their underlying hypotheses about the nature of an immunogenic epitope, its elements, interrelationships and system boundaries. These include restricting epitopes to the solvent accessible and exposed (i.e., top) external domains of the mature protein that must be to the same class and position to distinguish self from non-self. Eplets now displayed in EpR have limited experimental confirmation and close examination of 'confirmed' complex eplets reveals that usually only one among multiple AA is confirmed by absorption/elution, while all others within the eplet are based on older reports using non-specific techniques and not confirmed. To overcome perceived limitations of these models, we developed a third independent reverse engineering method in which software performed unbiased triplet scanning of every transcribed exon in the full length (leader included) proteins of every locus and identified triplet regions (clusters) shared by all primary transplant recipients making the same DSA. Once clusters defined the range and reaction patterns of the HLA disparate recipients were analyzed, alignment to IMGT easily allowed identification of target AA recognition sites.

Our data call into question some of the assumptions of current models revealing they impose limitations obscuring features of the

target HLA molecules that appear to be important. We found that not only solvent accessible, exposed, AA of the mature protein are targets for DSA development. Uniform reactivity to particular clusters and AA (1) underlying the peptide, (2) in domains encoded by exons 4, 5, 6 and 7 (alpha 3, TM, and Cyto domains) for some class I DSA, and (3) by exons 1 and 4 (leader and alpha 3 domain) for many class II were observed. Apart from leader targets, both the Terasaki and Duquesnoy groups also observed these types of reactivity, described by El-Awar, et al. [5] as "cryptic" (e.g., 74H for A2), or listed with low or very low ElliPro scores in EpR. The designation of 'cryptic' was based on the absence of reactivity to untreated beads and presence of reactivity to acid treated beads. However, Figs. 11, 12 of their report, show reactions of ~1000 MFI for the 'cryptic' epitopes with the highest reactivity for the untreated beads at ~8000 MFI (a narrow dynamic range). Using our cutoffs and a much greater dynamic range, we would consider their 'cryptic' epitopes positive. Further, in our view, labeling an epitope as cryptic using artificial experimental conditions does not obviate the potential for it to be a legitimate DSA target in an actual biological setting where there can be ischemic injury. Both other systems discounted targets in the alpha 3 domain based on their models because they were at the 'bottom' of the molecule, "not exposed at the surface of the HLA molecule," and presumed inaccessible [4,12]. This contrasts with our data where there is uniform reactivity by every recipient making DSA to these target AA. Further, AA in the transmembrane or cytoplasmic regions can alter the solvent exposed orientation of the molecule and/or create a soluble molecule. Interestingly, we found DSA to leader sequence targets did not occur in the class I DSA we analyzed but their frequent presence among class II suggests that the leader and not just the mature protein becomes exposed to the immune system. There is precedence for this as has been described for HLA-E, and other HLA molecules are known to present HLA peptides (e.g., B27) [18,19]. Given that there is constant cell turnover and death, the release of exosomes decorated with HLA, misfolded proteins which undergo degradation, and that we find the same target AA in every recipient making a particular DSA, it appears too simplistic to consider only solvent exposed portions of mature HLA molecules in their native configuration as potential DSA targets.

Alternative explanations would be that somehow finding these epitopes is (1) a function of the SAB or (2) not including data from labs that didn't pass the QC. In the first instance, SAB are coated with intact complete HLA antigens including the transmembrane and cytoplasmic domains, are produced in a human cell line and normally processed. Thus, the beads represent a native form of HLA (and randomly processed peptides) and it is possible, using these beads with our algorithm, to recognize epitopes present in other parts of the molecule than only the solvent exposed portion. Importantly, however, the epitopes we found were present in every randomly matched primary transplant recipient making any given DSA. Thus, these are actual biologically relevant results (not artefact) because the reactivity occurred in response to the transplant and the DSA was to the target HLA on the organ and cells in whatever conformation that exists (native/denatured). We are seeing how their immune systems reacted to the mismatched donor antigens without bias. Consequently, it is exceptionally difficult to explain why EVERY recipient making the same DSA sees the exact same cryptic 'artefactual' epitopes and that these have no biological relevance, particularly since we did not find DSA epitopes at every polymorphic site in these regions. In the second instance, the exclusion of data not meeting the 80% concordance threshold using 1000 MFI as a cutoff means that perhaps some recipients were not assessed because their DSA was below the threshold. That, however, should not have compromised the reliable data we did obtain in the way including weak (+/−) reactions might have.

For our analyses, we did not distinguish reactivity by IgG only, C1q only, or both, since the concordance for the 64 DSA triplets and 113 target AA was 100% for the 9 alleles reactive by both methods. We also did not investigate the IgG subclasses and C1q+ only isotypes in this study. However, the bulk of the results came from transplant pairs submitted by Stanford (241/332) and we have previously performed binding studies on 'C1q+ only' antibodies with different second step antibodies and shown them to be IgM with a single exception. Related to this was a report by Chen [20] showing competition between IgM and IgG on the SAB. It is possible that there is more IgG reactivity than we observed given this report with respect to IgM; however, we did not do titers nor did we pretreat the sera with EDTA or DTT. It would be extremely unusual if this IgM blocking mechanism were operating in the current study because for some DSA targets (B8, n = 7; Cw7, n = 8), we detected only C1q positivity with no IgG. It would be extraordinary for all patients making the same DSA to display this type of blocking reactivity.

Our descriptions of potential epitopes in cryptic, leader, or TM and cytoplasmic domains run counter to current models (which also found some of these), but we view it important to report what we found and not discount or eliminate from consideration results that we currently have no models to explain. Our findings provide an opportunity for multiple studies by those who wish to review/study our fully reported data and design experiments to test the various models or offer explanations about why targets (epitopes?) in cryptic or sequestered regions might be reacting, important, and clinically relevant (or not). Our view is that if we (collectively) don't look or are reluctant to investigate what we don't understand, we will not find potentially important features of the antibody/antigen interaction and epitopes in much the same way that high resolution typing of HLA using only exons 2 and 3 of class I does not reveal the whole picture of polymorphism.

Our ability to define precise AA epitopes using reverse engineering is particularly important for DQ DSA because, as previously noted [10,21], unless analyzed separately, it is difficult or impossible to assign the epitopes since targets reside on both chains. In the IHIWS cohort, we could clearly distinguish DQA from DQB DSA in numerous cases allowing the precise definition of chain specific clusters and target AA. This may account for some of the differences observed between our method, TerEP, and EpR such as we observed for DQ2 where mapping suggests combinatorial recognition sites (e.g., a2 and b4 on the alpha and beta chains, respectively) and others unique to one chain (e.g., a3-a6 on the alpha chain only).

Our data do not require a 'self' component to explain DSA formation but do not directly address this. In only 5/16 DSA groups was it necessary to invoke recognition of several nearby AA (no 'self' residues included) acting together as a target to explain reactivity (12 of 172 AA targets). Perhaps the existence of clusters might indicate some support for this concept but the target AA epitopes we defined appear sufficient to explain the immunogenicity.

There is a high probability that true antibody inducing AA epitopes are defined when all three models coincide. Outliers appear to be sample, method and hypothesis dependent. For example, no DQA1*01 epitopes are listed (likely not tested) as TerEp, but 17/30 (56.7%) DQA1*01 target AA are shared by EpR and our method. Disparities in DQ6 appear to be the result of the target allele with TerEP defining epitopes for DQB1*06:01 which are quite different than the DQB1*06:02/:04/:09 group we analyzed. We also found that IgG and C1q testing both identify the same target triplet clusters and AA (including cryptic sites), although not all IgG + DSA are complement fixing or vice versa. Cytotoxic epitopes are not identified in the TerEP model because testing was performed by binding assays.

Not all polymorphic sites in IMGT are identified by our reverse engineering algorithm as DSA targets suggesting that it is not simply substantial polymorphism that creates an immunogenic epitope. Thus, there is no *a priori* way to define an epitope from sequence data with certainty. Definition of epitopes clearly depends on the alleles of recipient and immunizer. Missing, inconsistent, or spurious epitopes may be a function of the number of individuals tested or whether only a monoclonal was used or the model itself. The use of monoclonals, representing a single clone's reactivity to a single allele (without high resolution sequencing of responder and immunizer) could generate a library of very unique epitopes related to the exact pair that are not generalizable to the

population, particularly when using murine monoclonals. Based on their data, El-Awar, et al. [4] noted that some epitopes causing an immune response in mice may not trigger the same immune response in humans. Our findings indicate that unless large high resolution typed human cohorts with the same DSA are tested, such that an unbiased mix of alleles is represented, common epitopes cannot be clearly defined. Many complex TerEP and EpR epitopes/eplets, based on modeling with limited experimental data, also contain AA that our data suggest are not generalizable and may be unique to the responding pair.

Finally, our study investigated potential epitopes in patients making the same DSA. We did not study outcomes nor do our data provide information about the minimum number of epitopes required for DSA generation or their relative immunogenicity. We do not presume to know what causes AMR (since there is DSA negative AMR) or what induces it or when. It is certainly conceptually easy to visualize that during the transplant itself when vessels are cut, or when there is ischemia reperfusion injury, cell membranes will be compromised and 'cryptic' portions of HLA molecules could be exposed as epitopes. These would be important future studies.

5. Conclusion

By analyzing triplets uniformly recognized in any given DSA group, tabulating which cells react and which do not, and comparing the reactivity to IMGT sequences, we have defined the exact target AA epitopes and described which epitope targets responders do not make antibody to, depending on their own alleles. The presence of uniform clusters and target AA revealed by reverse engineering in every random transplant pair making a particular DSA provides a high level of confidence in the defined AA targets being essential to the formation of antibody, although any given individual may only be able to respond to a subset of these. Using the algorithm provides the opportunity to perform focused studies of cohorts making particular DSA to expand the knowledge we have gained here. The future challenge for the field will be to develop a common, informative (hopefully, simple) nomenclature for HLA epitopes to facilitate discovery and discourse. Inclusion of the allele and chain (if applicable) of origin together with AA position would be highly desirable.

Acknowledgements

The authors wish to acknowledge the excellent work of the nine centers submitting complete data for analysis to the 17th IHIWS. These were: Australian Red Cross Blood Service, Blood Transfusion Center of Slovenia, Bloodworks NW, General Hospital of Athens, Hospital Universitario Cajuru, Johns Hopkins University, Mayo Clinic (Wisconsin), Stanford University, University of Chicago. The authors are grateful for the participation of One Lambda, Inc (a division of ThermoFisher) and Illumina in supplying standard reagents for use in the studies and for financial support of the 17th IHIWS by the Stanford Blood Center. This research did not receive any specific grant from funding agencies in the public, commercial, or not-for-profit sectors.

Declarations of interest

None.

Appendix A. Supplementary data

Supplementary data to this article can be found online at https://doi.org/10.1016/j.humimm.2019.04.004.

References

[1] S.G.E. Marsh, J.G. Bodmer, Hla-Dr and Hla-Dq Epitopes and monoclonal-antibody specificity, Immunol. Today 10 (1989) 305.
[2] N. El-Awar, J.H. Lee, C. Tarsitani, P.I. Terasaki, HLA class I epitopes: recognition of binding sites by mAbs or eluted alloantibody confirmed with single recombinant antigens, Hum. Immunol. 68 (2007) 170.
[3] N.R. El-Awar, T. Akaza, P.I. Terasaki, A. Nguyen, Human leukocyte antigen class I epitopes: update to 103 total epitopes, including the C locus, Transplantation 84 (2007) 532.
[4] N. El-Awar, A. Nguyen, K. Almeshari, M. Alawami, F. Alzayer, M. Alharbi, et al., HLA class II DQA and DQB epitopes: recognition of the likely binding sites of HLA-DQ alloantibodies eluted from recombinant HLA-DQ single antigen cell lines, Hum. Immunol. 74 (2013) 1141.
[5] N. El-Awar, P.I. Terasaki, J. Cai, C.-T. Deng, M. Ozawa, A. Nguyen, et al., Chapter 24 Epitopes of HLA-A, B, C, DR, DQ, DP and MICA Antigens, Terasaki Foundation Laboratory, Los Angeles, California, 2014.
[6] R.J. Duquesnoy, HLAMatchmaker: a molecularly based algorithm for histocompatibility determination. I. Description of the algorithm, Hum. Immunol. 63 (2002) 339.
[7] R.J. Duquesnoy, A structurally based approach to determine HLA compatibility at the humoral immune level, Hum. Immunol. 67 (2006) 847.
[8] R.J. Duquesnoy, A. Mulder, M. Askar, M. Fernandez-Vina, F.H.J. Claas, HLAMatchmaker-based analysis of human monoclonal antibody reactivity demonstrates the importance of an additional contact site for specific recognition of triplet-defined epitopes, Hum. Immunol. 66 (2005) 749.
[9] R.J. Duquesnoy, M. Marrari, A. Mulder, Usefulness of the nonself-self algorithm of HLA epitope immunogenicity in the specificity analysis of monospecific antibodies induced during pregnancy, Front. Immunol. 6 (2015).
[10] C.S.M. Kramer, D.L. Roelen, S. Heidt, F.H.J. Claas, Defining the immunogenicity and antigenicity of HLA epitopes is crucial for optimal epitope matching in clinical renal transplantation, Human Leukocyte Antigens 90 (2017) 5.
[11] R.J. Duquesnoy, M. Marrari, Correlations between Terasaki's HLA class I epitopes and HLAMatchmaker-defined eplets on HLA-A,-B and-C antigens, HLA 74 (2009) 117.
[12] N. El-Awar, et al., Epitopes of HLA-A, B, C, DR, DQ, DP and MICA antigens, Clin. Transpl. 2009 (2009) 295.
[13] R.J. Duquesnoy, M. Marrari, HLAMatchmaker: a molecularly based algorithm for histocompatibility determination. II. Verification of the algorithm and determination of the relative immunogenicity triplet-defined of amino acid epitopes, Hum. Immunol. 63 (2002) 353.
[14] R.J. Duquesnoy, M. Marrari, L.C. da M Sousa, J.R. de M Barrosa, K.M. de S U Aita, A.S. da Silva, et al., 16th IHIW: a website for antibody-defined HLA epitope Registry, Int. J. Immunogenet. 40 (2013) 54.
[15] M. Marrari, R. Duquesnoy, Correlations between Terasaki's HLA class II epitopes and HLAMatchmaker-defined eplets on HLA-DR and-DQ antigens, HLA 74 (2009) 134.
[16] V. Kosmoliaptsis, T.R. Dafforn, A.N. Chaudhry, D.J. Halsall, J.A. Bradley, C.J. Taylor, High-resolution, three-dimensional modeling of human leukocyte antigen class I structure and surface electrostatic potential reveals the molecular basis for alloantibody binding epitopes, Hum. Immunol. 72 (2011) 1049.
[17] D.H. Mallon, J.A. Bradley, P.J. Winn, C.J. Taylor, V. Kosmoliaptsis, Three-dimensional structural modelling and calculation of electrostatic potentials of HLA Bw4 and Bw6 epitopes to explain the molecular basis for alloantibody binding: toward predicting HLA antigenicity and immunogenicity, Transplantation 99 (2015) 385.
[18] L.L. Lanier, Follow the leader: NK cell receptors for classical and nonclassical MHC class I, Cell 92 (1998) 705.
[19] T.S. Jardetzky, W.S. Lane, R.A. Robinson, D.R. Madden, D.C. Wiley, Identification of self peptides bound to purified HLA-B27, Nature 353 (1991) 326.
[20] G. Chen, F. Sequeira, D. Tyan, Parallel C1q and IgG assays on single antigen beads reveal that the presence of IgM complement fixing antibodies can obscure clinically relevant IgG antibodies to the same allele, Hum. Immunol. 72 (2011) S12.
[21] A.R. Tambur, J. Rosati, S. Roitberg, D. Glotz, J.J. Friedewald, J.R. Leventhal, Epitope analysis of HLA-DQ antigens: what does the antibody see? Transplantation 98 (2014) 157.